ORNL-3231
UC-80 – Reactor Technology

# ARMY REACTORS PROGRAM

# PROGRESS REPORT

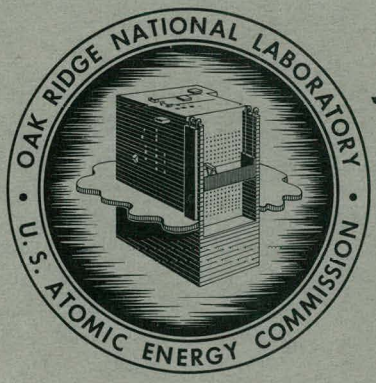


**OAK RIDGE NATIONAL LABORATORY**
operated by
UNION CARBIDE CORPORATION
for the
U.S. ATOMIC ENERGY COMMISSION

## DISCLAIMER

Printed in USA. Price $1.50. Available from the
Office of Technical Services
Department of Commerce
Washington 25, D.C.

ORNL-3231

UC-80 – Reactor Technology
TID-4500 (16th ed.)

Contract No. W-7405-eng-26

# ARMY REACTORS PROGRAM PROGRESS REPORT

L. D. Schaffer
Program Coordinator

DATE ISSUED

FEB 14 1962

OAK RIDGE NATIONAL LABORATORY
Oak Ridge, Tennessee
operated by
UNION CARBIDE CORPORATION
for the
U. S. ATOMIC ENERGY COMMISSION

THIS PAGE

WAS INTENTIONALLY

LEFT BLANK

CONTENTS

THIS PAGE

WAS INTENTIONALLY

LEFT BLANK

ARMY REACTORS PROGRAM
PROGRESS REPORT

## Summary

The Laboratory's participation in the Army Nuclear Power Program continued to include consultation, inspection, and general support in various areas of pressurized-water reactor technology. A large part of this effort was devoted to research and development work on metallurgical aspects of pressurized-water systems.

A survey was made of the methods of determining fuel burnup. Two recommendations for reporting fuel burnup resulted from this work. For low-enrichment fuels where an appreciable fraction of fissions occur in plutonium, the recommended means for reporting fuel burnup is fission density. For highly enriched fuels the preferred means of reporting burnup is per cent depletion.

The mechanisms and kinetics of the loss of boron during heating at 1135°C in various dynamic environments were determined. Powder compacts of 5 wt % elemental boron in various metals and oxides were heat treated in vacuum, high-purity argon, wet helium, and hydrogen. The loss mechanism in the environments other than hydrogen is thought to involve oxidation and volatilization of the boron influenced by the structure of the compact and by the sintering environment. Loss of boron in hydrogen occurred without significant influence of the matrix material or of the water content of the hydrogen. The loss mechanism in hydrogen is postulated to be a hydrogen-boron reaction resulting in a gaseous product. Compacts of 0.25 wt % boron were heat treated at varying times in hydrogen which contained three water vapor levels. The rate of sample sintering appeared to have a proportional effect on the boron loss. The loss appeared to be controlled by the rate of diffusion of the gaseous reactants in and the reaction product out of the sample. Wrought specimens of 0.13 wt % boron-stainless steel alloy were tested in helium and hydrogen. The rate of loss in these specimens is controlled by the rate of solid-state diffusion of boron to the gas-metal interface, assuming that the gas can react with the boron at the interface to maintain a low boron surface concentration.

In order to improve the distribution of $UO_2$ in the stainless steel matrix of the $UO_2$-dispersion-type fuel plate, a model has been developed to quantitatively characterize the $UO_2$ dispersion microstructure of roll-clad fuel plates relative to an "ideal" dispersion. Two indexes have been formulated. The over-all index characterizes the $UO_2$ as to the amount of fragmentation that occurred during the fabrication, and the stringering index indicates the extent of particle stringering that occurred. Using this method of dispersion characterization, a comprehensive study of the processing variables which affect dispersion quality is planned.

In order to avoid the loss of boron from $UO_2$-stainless steel dispersion fuel plates during fabrication, studies have been carried out on a refractory glass containing 4 wt % $B_2O_3$. This material has shown considerable merit. It resists stringering in the fuel matrix at the fuel plate rolling temperature and shows no reaction with the stainless steel or $UO_2$. Compacts and plates containing this boron glass in burnable poison proportions were fabricated, and the postfabrication boron analysis showed no boron loss.

By using low-silicon elemental powder, the undesirable reaction between $Eu_2O_3$ and Si was eliminated; and 13 full-size SM-1 type absorbers were fabricated at ORNL. However, since this time, other fabricators have encountered a new swelling problem with the $Eu_2O_3$-stainless steel matrix during fabrication. Therefore, additional studies have been undertaken to explore this problem and the recently discovered problem where 30 and 40% $Eu_2O_3$ specimens have shown unsatisfactory corrosion behavior. Sintering studies have been performed on the $Eu_2O_3$ powder to study such variables as powder preparation, sintering environment, powder-environment reactions, and the volatile constituents in the powder. The possibility of improving the corrosion properties of $Eu_2O_3$ by stabilizing the cubic phase of $Eu_2O_3$ is being studied along with the general corrosion behavior of $Eu_2O_3$ compacts at varying temperatures in $H_2O$. Furthermore, the stability of $Eu_2O_3$ in silicon-bearing stainless steel is being investigated.

Work has continued on the boron-gradient neutron absorber concept. In the original irradiation test work on the 3% enriched boron (92% $B^{10}$) dispersion in iron, it was found that this material could withstand a

burnup of 4% of the $B^{10}$ atoms. Because of the self-shielding character of boron, the surface burnup of this sample was as high as 30 at. %. In order to circumvent high localized burnup and the associated material damage, the boron loading was gradated in the compact. A full-size absorber based on this design was prepared for irradiation testing in SM-1.

In order to reduce the cost of the $Eu_2O_3$-stainless steel absorber and to increase the useful life of the boron gradient control rod, a design has been under study for preparing a composite control rod having the upper section made of a boron-gradient dispersion and the lower tip made of $Eu_2O_3$ and stainless steel. Full-size plates have been prepared. Preparation of a control rod based on this design for testing in SM-1 is now in progress.

Two fuel elements have been examined after significant exposure in SM-1. As reported previously, fuel element No. 72, removed after 10.5 Mwyr of reactor operation, was examined. The measured $U^{235}$ depletion was an average of 16% and a maximum of 30%. The element was dimensionally stable except for rippling of the outer fuel plates. Significant brazed-joint corrosion was noted, and a small number of intergranular cracks were observed in the cladding of some of the fuel plates. Fuel element No. 79, which operated 16.4 Mwyr in SM-1, was also examined at ORNL. The average $U^{235}$ depletion was 42%, and the peak depletion was 57%. No sign of gross deterioration or cracking was noted in the fuel matrix. The assembly was dimensionally stable, and the brazed joint corrosion did not appear to have degraded further than previously noted in element No. 72. The intergranular cracks noted in element No. 79 were much more numerous than in element No. 72, and some transgranular cracking was seen which had not been noted previously.

The examination of the miniature boron-iron samples in the final phase of the MTR irradiation test has been performed. The results show general agreement with data previously reported on the full-sized sections removed from SM-1.

In support of the $Eu_2O_3$-stainless steel control rod development program, 12 miniature test specimens containing 20, 30, or 40 wt % $Eu_2O_3$

were placed in the ETR for test. Six specimens have been removed that received unperturbed, integrated, thermal-neutron flux exposures of up to $14.8 \times 10^{20}$ neutrons/cm$^2$. No dimensional changes were noted, and the microstructure of the dispersions appeared to be unaltered.

Postirradiation testing of intentionally defected $Eu_2O_3$ dispersion samples has been performed. It was found that radiation exposure has a slight effect on reducing the corrosion resistance of the compact, but the amount of $Eu_2O_3$ incorporated in the dispersion has a more significant effect than the irradiation.

A control rod rack made of 17-4 pH stainless steel was removed after being operated in the SM-1 reactor for three years. The rod was inspected for cracks, sectioned, and examined metallographically. No defects were found.

Surveillance specimens of ASTM A-212, grade B, steel have been removed from the SM-1 reactor and tested at ORNL. The results indicate that the transition temperature of this material has shifted 36°F at the upper end of the test bar. This shift increases down the bar as the integrated fast-neutron flux increases, and at the lower end of the bar the shift was found to be 138°F.

# 1. REVIEW AND GENERAL SUPPORT

As part of the Army Reactors Program at ORNL, an attempt is made to maintain a general awareness of the activities and current problems in the Army Reactor programs so that consultation and support can be readily provided when requested by the Division of Reactor Development, Army Reactors. During the current report period such assistance was provided on a variety of problems requiring short-term efforts of several members of the Laboratory staff. The more significant activities of this nature are discussed here.

## SM-1 Support

After core I of the SM-1 had reached its end of life (16.4 Mwyr on April 28, 1960), the fuel elements were rearranged and several new fuel elements were added. In the rearrangement operation the caps were removed from the control fuel baskets and the $Eu_2O_3$ control rods were withdrawn for inspection. During this inspection, it was discovered that the control rod in shim position 2 was stuck in its basket. ORNL was requested to participate in the investigation of this problem. Close visual examination showed that the $Eu_2O_3$ control rod was in good condition and that the rod sticking was due to the basket having been deformed inward in the vicinity of the cap slots just above the control rod. The control rod was freed from the basket; the basket was repaired; and the control rod was reinserted into the reactor.

The modified core was then operated until April 15, 1961, the end of its life. It achieved a total power production of 17.98 Mwyr. In this modified core, which consisted mainly of core I fuel elements, there were three high-burnup fuel assemblies which were being considered for placement in core II. These elements, along with the five $Eu_2O_3$ control rods, were inspected by ORNL personnel. No signs of difficulties were noted in any of these components during the visual examination. ORNL recommended that the five $Eu_2O_3$ control rods be retained in core II. In addition, since the postirradiation examination of the two SM-1 fuel elements removed

at 10-Mwyr exposure did not show any effects to cause concern over the general stability of these fuel elements, ORNL also recommended that any two of the three high-burnup elements be reinserted into the reactor with core II.

Since the $U^{235}$ burnup limitation of these fuel elements and, therefore, the likely modes of fuel element failure are not known, arrangements were made to expedite examination of the irradiated SM-1 fuel elements at ORNL. The detailed examination of element No. 79 (16.4-Mwyr exposure) revealed that the cladding was beginning to show what appeared to be stress cracks. Since there is no evidence to show how far these cracks could propagate, ORNL recommended that the high-burnup fuel elements be removed from the SM-1 reactor until the significance of this cracking can be established. The removal was accomplished during October 1961. It was further recommended that, if circumstances preclude further testing in the SM-1, consideration should be given to testing one of these high-burnup elements to failure in a GETR loop.

An SM-1-type assembly containing 14 fuel tubes of the PM-1 design failed after 2 Mwd of operation in SM-1. The failure involved two fuel tubes that blistered and released fission products to the reactor coolant. ORNL personnel assisted in reviewing and making recommendations on this problem. The failure was found to be caused by water logging. The fuel element was redesigned, and recent tests indicate that the modifications which were made have eliminated the elements' susceptibility to failure by water logging.

Two spare SM-1 fuel elements that require reworking were sent to ORNL. While in storage at SM-1, it was noted that one element had a dent in the end box and another assembly was dirty. These elements were repaired, cleaned, and returned to SM-1.

## Code Development Program Review

Consulting service for the Army's Code Development Program continued to be provided. In this program The Martin Company is developing an integrated system of nuclear reactor codes which should be a very useful

analysis tool. The usual stepwise analysis procedure (i.e., multigroup slowing-down flux determination, reduction to few groups, homogenization of cells, full-core reactivity determination, reactor burnup) will be handled in a single turn at the computer with a consequent substantial reduction in the over-all time required for reactor analysis.

In the synthesizing of this so-called Pilot Code, emphasis has been placed on the utilization of existing codes written in the Fortran machine language rather than on the writing of new codes. In support of the code development program is a critical experiment program aimed at generating experimental data over a wide range of metal-water ratios and over a wide range of boron and $U^{235}$ fuel loadings that may be of interest in future SM-1-type reactor designs. The critical experiment data, therefore, should serve to test the range of applicability of the Pilot Code, as well as to suggest areas of future code improvement.

ORNL participation in this program consisted of reviewing technical reports prepared by The Martin Company, attending quarterly information meetings, and providing technical consultation to the Division of Reactor Development, Army Reactors. Our main influences on this program have been:

(1) to encourage the design and execution of experiments which would critically test the analytical methods (e.g., fine thermal and epithermal flux distributions through a fuel element, homogeneous-heterogeneous fuel element substitution, and measurement of cadmium ratios throughout the core),

(2) to encourage interaction of analytical and experimental efforts by rapid analysis of experimental data,

(3) to encourage the inclusion of an option in the Pilot Code to compute the effective delayed-neutron fractions that are useful in the analysis of certain critical experiment data, and

(4) to assure that each part of the Pilot Code give consistent treatment of geometry and physics.

## General Support

Core I of SM-1A arrived at Fort Greely, Alaska, June 16, 1960. Upon inspection the core was found to have dents, scratches, and rippling in

the top and bottom fuel plates. At the request of the Division of Reactor Development, Army Reactors, an ORNL metallurgist visited Fort Greely to inspect this core. On the basis of this inspection, the reactor designer, Alco Products Incorporated, recommended rejection of seven of the fuel elements. These are to be shipped to ORNL for further examination and disposition.

Consultation was provided on the fabrication of PM-2A core II and on the fabrication of $Eu_2O_3$ control rods for PM-2A and SM-1A. Evaluations and recommendations were made on the Army advanced fuel element development program for pressurized-water reactors, the hazards analysis procedure on SM-1, on the reactor control system of SM-1, and the reprocessing of SM-1 core I.

Additional efforts in the nature of consultation and design review were made for the Army program in general. ORNL authors presented two papers at the Army Nuclear Seminar last fall. These papers were: "Heterogeneous Control Rod Studies" by B. W. Colston, E. E. Gross, and M. L. Winton, and "Analysis of Reactor Excursions Terminated by Steam Formation" by R. S. Stone.

Pile period simulators were loaned to the SM-1 and SM-1A reactors. Transport carriers were provided for Army fuel shipments between SM-1, ORNL, BMI, and NRTS.

## 2. SURVEY OF METHODS OF DETERMINING FUEL BURNUP

R. L. Stover  G. K. Moeller
L. D. Schaffer

The burnup of nuclear fuel is generally understood to be a measure of the utilization of the fuel. Different viewpoints on the meaning of this utilization have resulted in various definitions of burnup.

An investigation of the various methods of representing burnup resulted in two recommended definitions:[1]

$$\text{Burnup in terms of fission density} \equiv \frac{\text{number of fission events}}{\text{volume } (\text{cm}^3) \text{ of fuel-bearing material}} , \qquad (1)$$

$$\text{Burnup in terms of per cent depletion of fissionable atoms} \equiv \frac{N^0 - N'}{N^0} \times 100 , \qquad (2)$$

where

$N^0$ = number fissionable atoms per $\text{cm}^3$ of fuel-bearing material before irradiation,

$N'$ = number fissionable atoms per $\text{cm}^3$ of fuel-bearing material after irradiation.

Fission density is of particular interest in low-enrichment uranium fuels because often an appreciable fraction of the fissions occurs in plutonium. Radiochemical analysis of fission products was found to be the most accurate method of determining fission density.

Percent depletion is of particular interest in highly enriched uranium fuels because it can be measured directly. It is most easily determined

---

[1] R. L. Stover and G. K. Moeller, Methods for Determining Fuel Burnup, MIT-OR-6, July 5, 1961.

from relative isotopic measurements before and after the irradiation. Isotopic ratios can be determined experimentally by a number of methods, the most accurate being mass spectrometry.

## 3. FUEL ELEMENT DEVELOPMENT

### Kinetics and Mechanisms of Deboronization

J. H. Cherubini

A basic study of the loss of boron from stainless steel matrices has been completed and reported.[1] The mechanisms and kinetics of the loss of boron during heating at 1135°C in various dynamic environments were determined from (1) powder compacts of 5 wt % elemental boron dispersed in matrices of Fe, Cr, Ni, Si, $Fe_2O_3$, $Cr_2O_3$, NiO, and $SiO_2$, (2) compacts of austenitic stainless steel alloy powder containing 0.25 wt % B, and (3) wrought specimens of 0.13 wt % B–stainless steel alloy.

The compacts containing 5 wt % B were heat treated in vacuum, high-purity argon, wet helium, and hydrogen. With the exception of those samples which were heat treated in hydrogen, significant boron losses occurred only when a supply of oxygen, either from the sample itself or as a deliberate addition to the heat-treating environment, was available. Correspondingly, the loss mechanism is postulated to be the oxidation of boron to boron sesquioxide and its volatilization from the sample. The loss rate is controlled by the volatilization rate of the oxide which is directly influenced by the structure of the compact and the sintering environment.

Independent of the chemical nature of the matrix, boron losses were incurred during heat treatment in hydrogen. Variations of the water content of the hydrogen from 7 to 460 ppm did not significantly influence the total boron loss observed. The synthesis of boron and hydrogen into a gaseous boron-hydrogen species is postulated as a predominating loss mechanism in the environment.

Compacts of austenitic stainless steel powder containing 0.25 wt % B were heat treated at 1135°C from 1/4 to 16 hr in hydrogen atmospheres of three different water vapor levels: 1, 100, and 460 ppm. The losses

---

[1] J. H. Cherubini, Determinations of the Mechanisms and Kinetics of Deboronization, ORNL-3141, Aug. 31, 1961.

observed in each environment for the first few hours of heat treatment followed the relationship:

$$\Delta B = 0.26\ t^{1/2} + C \quad , \qquad (1)$$

where

$\Delta B$ = total boron loss in mg,

$t$ = total heat-treating time in hr,

$C$ = a constant.

However, the rate of boron loss of samples heated in the driest hydrogen decreased abruptly after 2 hr at temperature. Under the other environmental conditions, a similar decrease was observed after 7 hr. The degree of sample sintering was found to be the predominant factor in determining the boron loss rate. The rate of decrease of total sample surface area by sintering was observed to have a proportional effect in decreasing the rate of boron loss.

The rate-controlling step in the deboronization of master alloy compacts was the rate of diffusion of gaseous reactant into and reaction products out of the sample. This in turn was controlled by the effective diameter, length, and number of channels permeating the compact and exposed to the sintering environment. Consequently, the variation of the heat-treating conditions affects the total boron loss only as it influences the rate of compact sintering.

The rate of deboronization of the wrought metal samples is controlled by the rate of solid-state diffusion of boron to the gas-metal interface, providing the heat-treating atmosphere can react with the boron at the interface so as to maintain a very low boron surface concentration. Deboronization of wrought specimens was observed in both hydrogen (less than 15 ppm $H_2O$) and helium (15 000 ppm $H_2O$).

## Improved Dispersions of $UO_2$ in Stainless Steel for High-Burnup Fuel Elements

J. H. Cherubini

The SM-1-type fuel elements consist of a series of plates containing 26 wt % $UO_2$ and 0.13 wt % $B_4C$ dispersed in stainless steel. The fuel is

prepared by hydrogen-firing hydrated $UO_3$ crystals at 1700°C. The irregular shape of this $UO_2$ and the roll-cladding method used in fabricating the composite plates are responsible for the general stringering and fragmentation of the fissile compound. Such a condition appears to be satisfactory to achieve the present design life of the SM-1 type of core. However, for the 70- to 100-Mwyr-life cores presently under consideration by Alco Products, Inc.,[2] it would be desirable to improve the distribution of $UO_2$ in the stainless steel matrix of the fuel plate so that the maximum spacing exists between centers of the dispersed phase particles. In this manner, the susceptibility of the fuel material to irradiation damage from overlapping zones of fission fragment recoil damage can be reduced.

Spheroidal $UO_2$ has been proposed as the fissile material for producing a microstructure with potentially superior radiation stability. Unfortunately, this type of oxide varies from batch to batch and a method of characterizing the quality of a particular dispersion relative to an "ideal" dispersion is needed to describe the microstructure of roll-clad fuel plates. A model for quantitatively characterizing $UO_2$ dispersions has evolved from recent studies.[3]

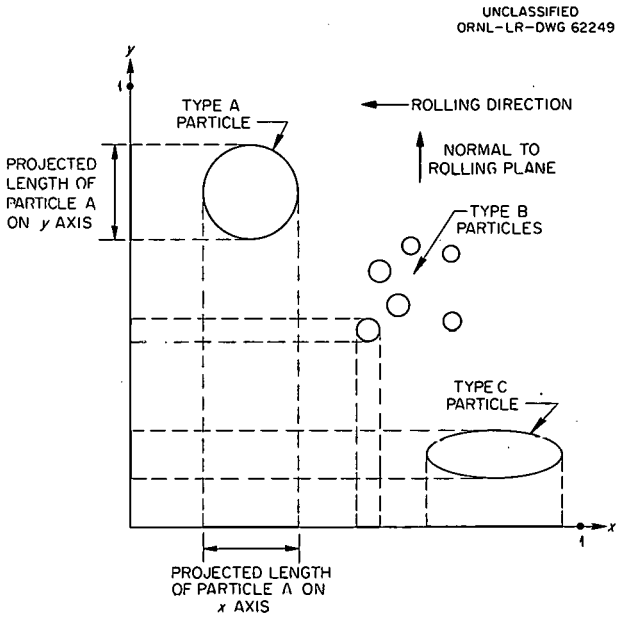


Fig. 3.1. Typical $UO_2$ Particle Geometries in Composite Plate Containing Dispersions of $UO_2$ in Stainless Steel.

Ideally, only three particle geometries need be considered in this model. As illustrated in Fig. 3.1, type A particles are spherical and have not been altered in the fabrication sequence; type B particles

[2] J. G. Gallagher, Ten Year Development Program for AEC-Army Reactors, AF Note 355, June 5, 1961.

[3] J. H. Cherubini, personal communication.

result from the fragmentation of parent particles and are discretely distributed throughout the matrix; and type C particles have been elongated in the rolling direction either by plastic flow or fracturing and stringering during the rolling process.

In the proposed method of indexing, a longitudinal microsection is examined and numbers, $\bar{x}$ and $\bar{y}$, proportional to the total length of particles projected on both the axis parallel (x) and perpendicular (y) to the rolling direction, are determined. The volume fraction (v) of the particles in the particular field of view is then established by a point-intercept method. Obviously, if the particles are ideal spheres, each particle appears as a circle and $\bar{x} = \bar{y}$, if stringered $\bar{x} > \bar{y}$. In order to compare indices from different dispersions and correct for localized inhomogeneities in a particular sample, the $\bar{x}$ and $\bar{y}$ values are divided by the volume fraction of dispersoid present yielding the empirical quantities, $\bar{x}_v$ and $\bar{y}_v$. The ideal index,

$$I = \frac{3v}{4R} \quad ,$$

which presupposes no particle degradation in the fabrication sequence, is calculated next. The average original particle radius is R. Then, the departure from ideality, $\bar{y} - I$, is a measure of the extent of dispersoid fragmentation and is directly related to the number of type B particles present. The stringering index, $\bar{x}_v - \bar{y}_v$, is directly related to the frequency of occurrence and extent of elongation in type C particles.

Photomicrographs of dispersions containing approximately 33 wt. % spheroidal $UO_2$ (-100 +140 mesh) in a matrix of type 347 stainless steel, reduced 87% in thickness at 1200°C by roll cladding, are presented in Figs. 3.2, 3.3, and 3.4. Each dispersion was fabricated in an identical manner, except that the first two samples were also cold rolled with 3.5% thickness reduction. Nevertheless, differences in dispersion quality are attributed to the particular lot of $UO_2$ contained in each sample. This relationship is quantitatively verified in Table 3.1. The dispersion suffering the greatest amount of stringering has an associated stringering index of 7.90; the intermediate, 3.38; and the best, 0.72. The over-all

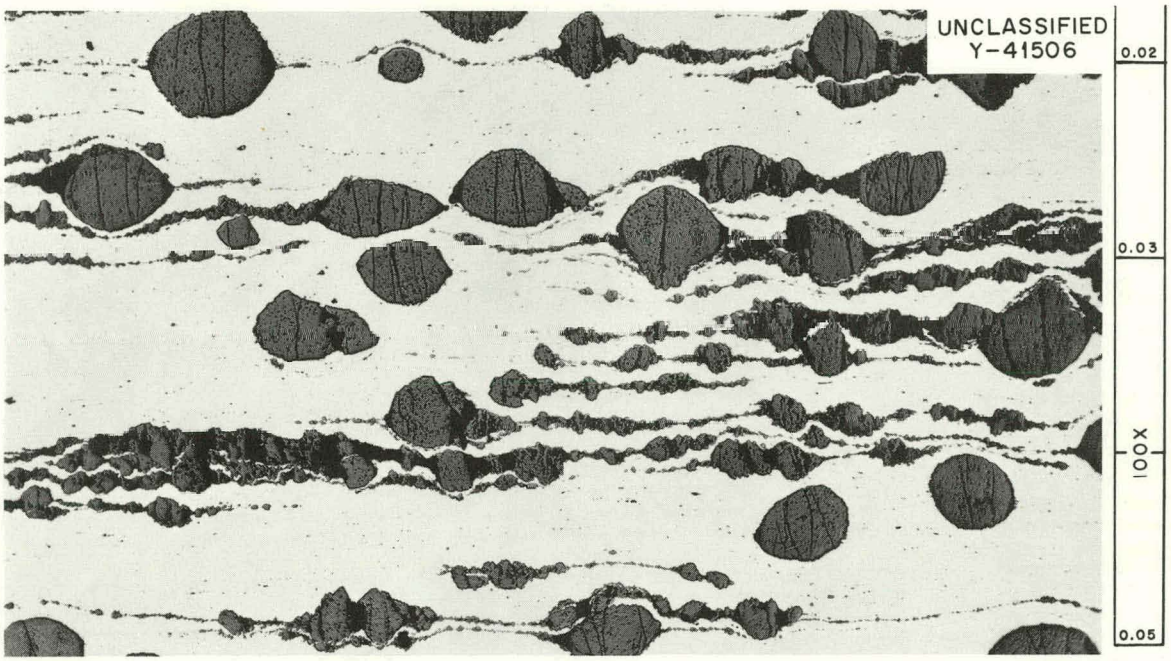


Fig. 3.2. Plate F128A Containing 35 wt % -100 +140 Mesh Spheroidal $UO_2$ (Batch J-01-EN) in a Matrix of Type 347 Stainless Steel. Cold rolled 3.5% after 87% hot reduction in thickness. As polished. 100X.

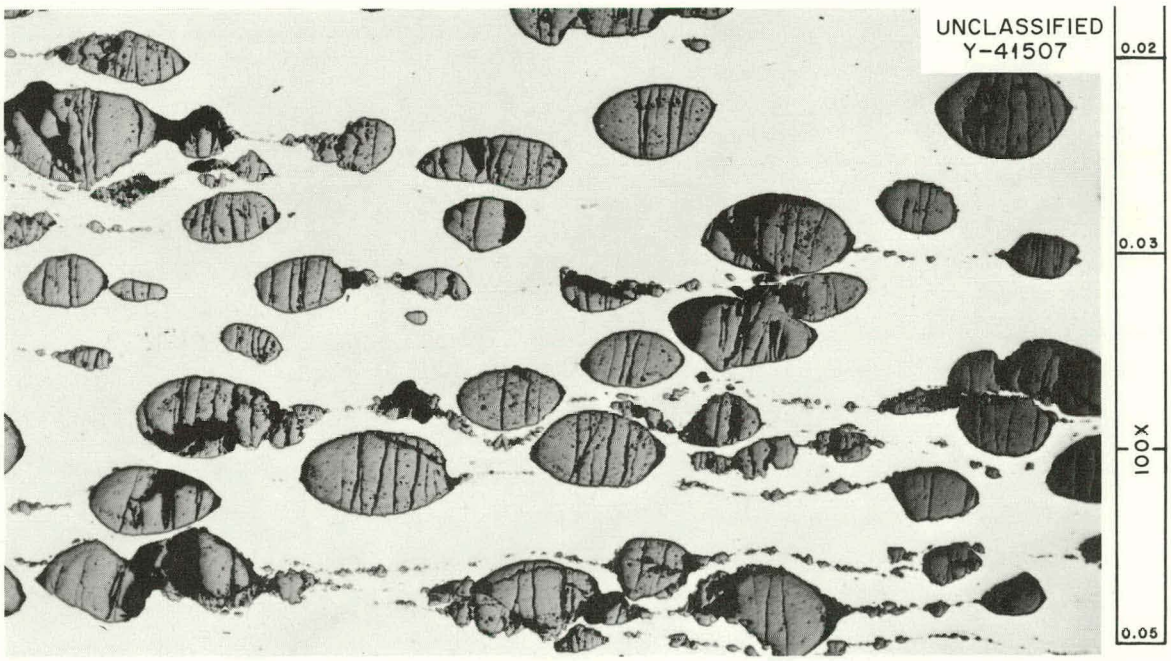


Fig. 3.3. Plate F131A Containing 35 wt % -100 +140 Mesh Spheroidal $UO_2$ (Batch J-07-EN) in a Matrix of Type 347 Stainless Steel. Cold rolled 3.5% after 87% hot reduction in thickness. As polished. 100X.

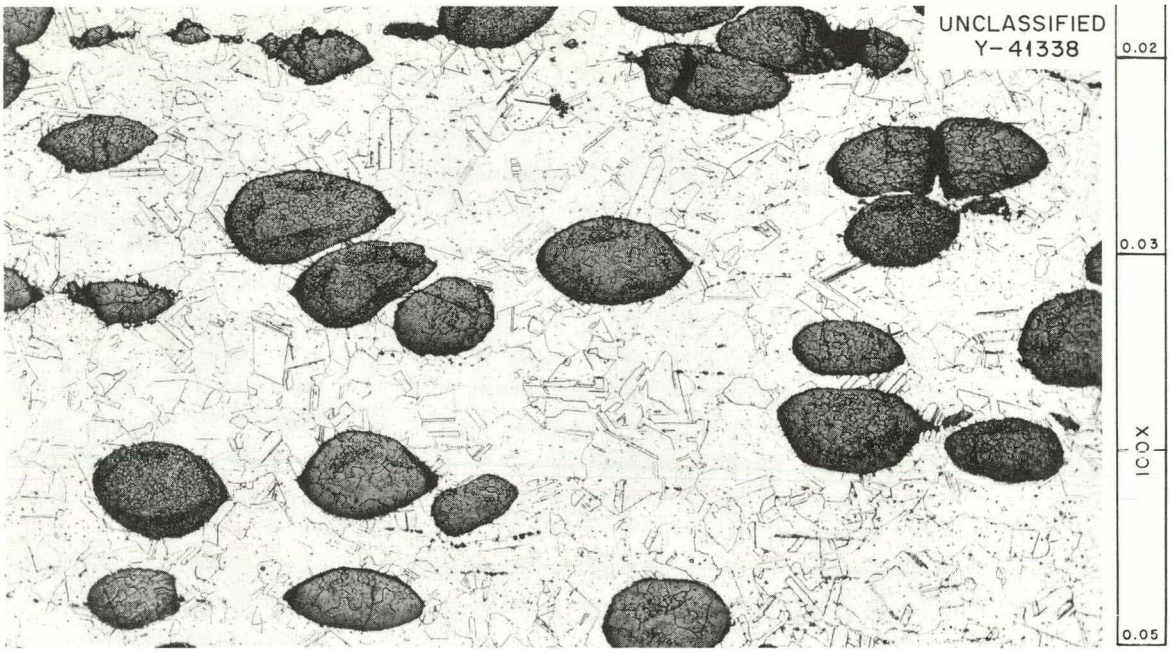


Fig. 3.4. Plate F282 Containing 35 wt % -100 +140 Mesh Spheroidal $UO_2$ (Batch H-03-HA) in a Matrix of Type 347 Stainless Steel. As hot rolled. Etchant: Glyceria regia. 100X.

Table 3.1. Fabricability Indices for Three $UO_2$ Dispersions

| Plate No. | Volume Fraction (v) | Mean Particle Diameter (mils) | I | $\bar{x}_y$ | $\bar{y}_v$ | Over-all Index $(\bar{y} - I)$ | Stringering Index $(\bar{x}_v - \bar{y}_v)$ |
|---|---|---|---|---|---|---|---|
| F128A | 0.336 | 2.6 | 1.02 | 10.25 | 2.35 | −0.23 | 7.90 |
| F131A | 0.395 | 2.6 | 1.19 | 5.68 | 2.20 | −0.32 | 3.38 |
| F282 | 0.240 | 2.6 | 0.73 | 4.10 | 3.38 | +0.08 | 0.72 |

indices of all three samples are equivalent and, judging from Fig. 3.3, the extent of fragmentation incurred is small. This indicates that, within wide limits of starting material quality, only a nominal amount of fragmentation is experienced by spheroidal $UO_2$ particles.

A comprehensive study of the processing variables which affect dispersion quality is planned using this method of dispersion characterization. In the area of powder metallurgical compact preparation, the variables to be studied include the effect of pressing and coining pressure and compact sintering. Cursory experiments indicate that, at least with

spherical oxides, green compacts produce fuel dispersions of comparable quality to those conventionally processed by sintering and coining. In addition, other experiments show that roll-cladding temperature and reduction schedule profoundly affect the dispersion morphology.

## Borosilicate Glass Burnable Poisons for Composite Fuel Plates

T. D. Watts

As reported previously,[3] all the boron-bearing compounds considered as potential burnable poisons in $UO_2$-stainless steel dispersion fuel plates have exhibited varying degrees of reaction with the austenitic steel matrix during fabrication in the temperature range from 1000 to 1200°C. Such reaction promotes erratic loss of boron from the fuel plates. Studies directed toward circumventing this problem have continued, and a refractory glass containing 4 wt % $B_2O_3$ has been shown to have considerable merit in the proposed application. Preliminary screening studies have indicated that this particular glass, in the form of spherical beads, will resist stringering at rolling temperatures high enough (1050°C) for fabrication of conventional APPR fuel plates. Glasses with higher $B_2O_3$ contents, such as ordinary pyrex (12 wt % $B_2O_3$), are extremely plastic at fuel plate fabrication temperatures and stringer severely.

Based on this favorable experience, further studies were undertaken to assure the compatibility of the glass with both $UO_2$ and type 347 stainless steel. Compacts and miniature roll-clad plates containing only glass beads in a type 347 stainless steel matrix were heat treated for times up to 24 hr at temperatures up to 1100°C. As expected, metallographic examination revealed no reaction. Several of the heat-treated compacts were chemically analyzed for boron. Within the accuracy of the analysis, there was no boron loss.

The actual compatibility between $UO_2$ and glass was not considered to be a very great problem, since most of the glass particles would be separated from the $UO_2$ particles by the matrix material, which comprises

---

[3]APPR Ann. Prog. Rep. Jan. 31, 1960, ORNL-2907, pp. 18–23.

approximately 70 vol % of the core. However, the probability of a glass particle being in contact with a $UO_2$ particle does exist. In order to facilitate a study of the effect of such contact, attempts were made to produce compacts without the stainless steel matrix. These compacts had no appreciable green strength and crumbled when ejected from the pressing die. It was, therefore, necessary to study the compatibility of glass and $UO_2$ in the presence of the stainless steel matrix. Compacts containing only 40 vol % matrix material were pressed and shown to have adequate green strength for handling. These compacts were roll clad at 1050°C and examined metallographically. Sufficient numbers of glass particles were in contact with $UO_2$ to reasonably evaluate the compatibility. Similar plates were then heat treated for periods up to 24 hr at temperatures up to 1100°C. These plates were examined metallographically, and no evidence of a reaction could be found.

During fabrication of miniature plates with the proposed SM-2 reactor fuel loading (38 wt % $UO_2$ + 0.4 wt % natural boron), many of the $UO_2$ particles fractured and stringered. This loading was predicated on using enriched $B^{10}$ in the glass. In a few cases, the $UO_2$ stringered around a glass particle, but in no instance did a glass particle break or stringer. Figure 3.5 is a typical photomicrograph showing glass particles in contact


Fig. 3.5. Core Structure in Annealed Fuel Plate Containing Boron-Bearing Glass Beads, $UO_2$, and Type 347 Stainless Steel. As polished. 200X.

with $UO_2$. A -170 +325 mesh size fraction was selected for both the fuel and poison. This plate had been annealed at 1100°C for 30 hr after rolling at 1050°C. The integrity of the glass beads and absence of reaction may be seen.

Chemical analyses of samples containing the SM-2 fuel loading with the boron in the form of refractory glass are presented in Table 3.2. These results include measurements on annealed compacts as well as rolled plates. Within the accuracy of the determinations, no boron loss is indicated.

Table 3.2. Boron Analyses of Miniature Fuel[a] Compacts After Various Treatments

Total boron charged: 0.0014 g
Weight of boron-containing glass: 0.1189 g

| Type of Sample | Total Boron Analyzed (g) |
|---|---|
| As-pressed compact | 0.0014 |
| Sintered and coined compact | 0.0015 |
| Heat-treated compact[b] | 0.0014 |
| Roll-clad compact[c] | 0.0014 |
| Annealed plate[d] | 0.0014 |

[a]Compacts contained 38 wt % $UO_2$ plus sufficient glass beads to give a boron loading equivalent to 0.4 wt % natural boron.

[b]Heat treatment was 24 hr at 1100°C.

[c]Rolling temperature was 1050°C.

[d]Plates were annealed 3 hr at 1150°C.

In view of the excellent stability and behavior of this material in a stainless steel matrix, studies will be continued with emphasis placed on a scale-up to full-size fuel plates.

# 4. CONTROL ROD DEVELOPMENT

## Europium Oxide Studies

R. A. McNees R. A. Potter

In the early phases of the development of europium oxide–stainless steel absorbers for the APPR program, one of the principal problems encountered was a reaction between the $Eu_2O_3$ and the silicon in the austenitic stainless steel.[1] This problem was thoroughly investigated and the results were recorded.[2] Use of low-silicon elemental metal powders circumvented the reaction problem and 13 full-size absorbers were ultimately fabricated with no difficulty.

However, when similar components were subsequently manufactured by commercial fabricators, a new and significant problem was encountered. The $Eu_2O_3$-stainless steel compacts swelled during the initial sintering step of the standard fabrication procedure[3] and created difficulty in the subsequent coining operation. This swelling was not believed to be associated with a europia-silicon reaction, since the level of silicon appeared to be acceptable on the basis of previous work. Studies were therefore undertaken to explore the mechanism of this swelling problem.

The unsatisfactory corrosion behavior in 300°C water of intentionally defective $Eu_2O_3$-stainless steel specimens containing 30 and 40 wt % oxide is also being investigated. Previous corrosion studies[4] indicated little attack of the dispersion in an aqueous medium; however, these results were obtained on a specimen containing 20 wt % $Eu_2O_3$ rather than 37 wt % $Eu_2O_3$, as erroneously reported. Techniques for overcoming this lack of corrosion resistance by stabilization of the cubic structure of $Eu_2O_3$ are being studied.

---

[1] APPR Ann. Prog. Rep. Jan. 31, 1960, ORNL-2907, pp. 23–27.

[2] C. F. Leitten, Jr., The Stability of Europium Oxide in Silicon-Bearing Stainless Steel, ORNL-2946, Aug. 9, 1960.

[3] C. F. Leitten, Jr. et al., Specifications and Fabrication Procedures on Europium-Bearing Absorber Rods for Reactivity Control in Core II of SM-1, ORNL-2733, July 29, 1959.

[4] APPR Ann. Prog. Rep. Jan. 31, 1960, ORNL-2907, pp. 30–32.

Sintering Behavior

Experiments have been conducted to study the effects of variations in powder history and sintering environment on the dimensional behavior of $Eu_2O_3$ at 1350°C. The underlying assumption in these studies is that, if the pure $Eu_2O_3$ compacts exhibit contraction on heating, similar behavior can be expected from dispersion compacts. The data listed in Table 4.1 describe the behavior of cylindrical compacts of three different types of $Eu_2O_3$ when heated to this temperature for 1 hr in air or in dry hydrogen. These data show that large volume changes occur when low-temperature calcined (800°C) cubic $Eu_2O_3$ is heated to 1350°C. The volume changes, coupled with the problems raised when blending the fluffy, cubic $Eu_2O_3$ with the metallic powders used in forming the core of the absorber plate, present a number of practical difficulties. Consequently, such a powder does not appear suitable, even though shrinkage during sintering is noted.

Table 4.1. Dimensional Changes of $Eu_2O_3$ Compacts After Heating to 1350°C for 1 hr

| Material[a,b] | Sintering Atmosphere | Dimensional Changes (%) | |
|---|---|---|---|
| | | Length | Diameter |
| A | Air | -4.3 | -6.3 |
| | Hydrogen | -5.2 | -5.2 |
| B | Air | -0.4 | -1.4 |
| | Hydrogen | +2.8 | +1.9 |
| C | Air | +0.4 | +0.3 |
| | Hydrogen | +1.6 | +0.6 |

[a] A — Powder, cubic form from calcination of $Eu_2(C_2O_4)_3$ at 800°C in air.

B — Powder, monoclinic form, after heating cubic powder to 1700°C in air for 3 hr.

C — Powder, monoclinic form, after heating cubic powder to 1700°C in hydrogen for 3 hr.

[b] Conditioning treatments for all three powders were performed several months prior to the present study. Compacts were cylindrical pellets, 1/4 × 1/4 in., pressed to 10 000 psi.

The behavior of the denser monoclinic powders prepared by heating the cubic form of $Eu_2O_3$ to 1700°C for 3 hr in either air or hydrogen indicates that the environment used during such heating probably does not determine the expansion behavior of compacts subsequently heated to 1350°C. In addition, the sintering atmosphere does not appear to be significant.

Another experiment was conducted to determine whether the particle size of the starting powder is a contributing factor in the expansion of $Eu_2O_3$ compacts during sintering. A portion of $Eu_2O_3$ from batch 10-1, which had been hydrogen-conditioned at 1700°C for 3 hr, was separated into four particle-size fractions. These fractions were used to prepare cylindrical compacts by cold pressing and heating to 1350°C in dry hydrogen for 1 hr. The changes in dimensions and weights are shown in Table 4.2. These data indicate that initial particle size is probably not an important factor in the expansion behavior of $Eu_2O_3$ compacts. On the other hand, the apparent correlation between the amount of weight loss from two of the compacts and their expansion behavior may be significant.

Table 4.2. Dimensional and Weight Changes in $Eu_2O_3$ Compacts Prepared from Sized Material Heated to 1350°C in Dry Hydrogen

| Size Fraction (mesh) | Dimensional and Weight Changes (%) | | |
|---|---|---|---|
| | Length | Diameter | Weight |
| As received | +3.0 | +3.8 | (a) |
| -60 +100 | +3.0 | +3.9 | (a) |
| -100 +270 | +3.3 | +2.8 | (a) |
| -270 +325 | +1.5 | +1.6 | -3.6 |
| -325 | +2.5 | +2.7 | -6.2 |

[a]Green compacts were too fragile to handle before heating. All compacts were very weak after firing.

In view of this possible correlation between weight loss and volume expansion of $Eu_2O_3$ compacts, an investigation was started of the volatile materials in $Eu_2O_3$ powder. A sample of oxide (batch 10-0), which had been air fired at 1700°C for 1 hr several months prior to use, was heated to

1450°C in a thermogravimetric apparatus at a pressure of approximately $10^{-5}$ mm Hg. A total weight loss of 8.4% was experienced, with almost all the loss occurring between 1050 and 1350°C. The rate of loss was barely perceptible at 1020°C but was very rapid at 1100°C, with indications that at 1060°C a marked increase in rate occurred. After samples had been heated at 1350°C until no further weight loss was observed, increasing the temperature to 1450°C resulted in no additional weight loss.

Samples of the oxide were taken before heating, after heating for only 10 min at 1100°C so that the reaction producing the weight loss had not been completed, and after heating to 1450°C. The x-ray diffraction pattern of the oxide before heating showed not only the expected monoclinic $Eu_2O_3$ pattern but also four additional peaks due to an "unknown phase" which was not cubic $Eu_2O_3$. After heating in vacuum to 1450°C only the monoclinic pattern remained, the four peaks due to the "unknown phase" having disappeared completely. The x-ray diffraction pattern of the sample of material that had been heated to 1100°C for 10 min showed, in addition to the monoclinic pattern, a reduced intensity of the "unknown phase" and the strongest peak of the cubic $Eu_2O_3$ pattern. It is postulated that the observed weight loss was due to decomposition of a compound such as europium hydroxycarbonate, with evolution of $CO_2$ and $H_2O$, and that, concurrent with this process, cubic $Eu_2O_3$ was produced which subsequently transformed slowly to the monoclinic form at 1100°C. It is generally accepted that the low-temperature body-centered cubic form of $Eu_2O_3$ transforms irreversibly to the monoclinic structure at temperatures above approximately 1050°C.

The plausibleness of this postulate as to the decomposition of a hydroxycarbonate is indicated by the chemical analyses of batch 10-0, a 1700°C air-conditioned powder, which contained 96.7% $Eu_2O_3$, and batch 10-1, a 1700°C hydrogen-conditioned oxide, which contained 95.5% $Eu_2O_3$. The presence of 0.4% carbonate was detected in both oxides several months after preparation. The temperature range over which a sample of oxide from batch 10-1 lost weight in vacuum was essentially the same as for oxide 10-0, although only a 5% weight loss was noted with the former after heating to 1450°C. In contrast to the vacuum heating behavior shown by oxides

10-0 and 10-1, a sample of $Eu_2O_3$ prepared only a week earlier, by calcination of $Eu_2(C_2O_4)_3$ in air at 1000°C for 2 hr, lost no weight in the temperature range from 1000 to 1400°C. The sample did show a 1% weight loss during initial evacuation and heating, presumably because of desorption of moisture.

The effects of sintering at 1230 to 1350°C for 1 hr in hydrogen on the behavior of hydroxycarbonate-contaminated $Eu_2O_3$ powder compacts is compared with the effects of such sintering on the behavior of the non-contaminated oxide compacts in the following statements:

1. A compact prepared from hydroxycarbonate-contaminated powder showed a diameter change of +3.0% and a weight change of −4.0%.

2. The same powder after heating to constant weight at 1450°C and a pressure of $10^{-5}$ mm Hg was compacted and when sintered showed a diameter change of +0.2% and a weight change of +0.05%.

3. Pure monoclinic $Eu_2O_3$ prepared by heating pure cubic $Eu_2O_3$ to 1750°C for 1 hr in $H_2$ was compacted and when sintered showed a diameter change of −0.2% and a weight change of +0.1%.

4. Pure monoclinic $Eu_2O_3$ prepared by heating pure cubic $Eu_2O_3$ to 1600°C for 1 hr in air was compacted and when sintered showed a diameter change of −2.0% and a weight change of +0.2%.

From these data, it appears that properly prepared $Eu_2O_3$ powder does not contain the hydroxycarbonate contaminant and that the powder that is contaminated can be made usable by heating to 1450°C at a pressure of $\sim 10^{-5}$ mm Hg.

The decomposition postulate is further strengthened by the results of differential thermal analysis of oxide 10-0. Two different heating rates, 10 and 25°C/min, were used at a pressure of approximately 1 mm Hg. During the 10°C/min heatup, an endothermic reaction was recorded from approximately 940 to 1250°C. At the more rapid rate of heating, the reaction started at approximately 1025°C and reached a maximum at approximately 1285°C. These observations indicate that the differential thermal analysis technique may be used to determine the pressure of hydroxycarbonate in $Eu_2O_3$ powder and to predict the sintering behavior of such powder.

One final point which evolved as a corollary to the sintering studies is also noteworthy. It was observed that pellets of $Eu_2O_3$ after being heated in a molybdenum induction furnace to 1600°C for 2 hr in hydrogen were completely covered with a yellow-orange crystalline deposit. The crystals were well developed, ranged in size up to 0.1 mm, and formed a loosely adhering crust over the surface of the pellets. Spectroscopic analysis showed that the crystals contained approximately 10% Si, although the powder from which the compacts were made contained less than 100 ppm Si. The same type of behavior, although less extensive, was observed in a molybdenum resistance furnace under the same conditions. Although the exact identity of the compound formed remains unsettled, it is apparent that $Eu_2O_3$ is a very efficient "getter" for any volatile, silicon-containing compounds formed in the furnace. Although no evidence for silicon contamination of the atmosphere had previously been found, the furnaces do contain some silicate-base insulating materials. It had been assumed, prior to this experience, that these insulating materials were not hot enough to allow for silicon volatilization in a hydrogen environment, but apparently this is not true. In light of the undesirable effects caused by silicon during fabrication of stainless steel-matrix absorber plates,[2] this observation points up the need for close control over all furnace equipment used in both $Eu_2O_3$ preparation and absorber plate fabrication.

## Aqueous Corrosion Behavior of $Eu_2O_3$

The possibility of improving the aqueous corrosion properties of $Eu_2O_3$ by stabilizing the cubic modification of the oxide has been suggested by the work of Shaeffer and Roy.[5] In the present study, stabilization of the cubic form to temperatures greater than 1100°C was attempted by heating a mixture of cubic $Eu_2O_3$–5 wt % cubic $Dy_2O_3$ to 1600°C in air for 1 hr. X-ray diffraction analysis showed the product to be a mixture of monoclinic $Eu_2O_3$ and cubic $Dy_2O_3$, which probably indicates the lack of reaction

[5]Rare-Earth Polymorphism and Phase Equilibria in Rare-Earth Oxides – Water Systems, J. Am. Ceram. Soc., 42(11): 563–70 (1959).

between the two starting materials. Under similar conditions using cubic $Y_2O_3$, the monoclinic form of $Eu_2O_3$ was again obtained. Further work on chemical stabilization of the cubic form of $Eu_2O_3$ is planned by using larger proportions of oxide additives, longer heating periods, and higher temperatures, as well as coprecipitated oxides for more intimate mixing.

In order to establish base-line behavior, the water corrosion behavior of five compacts of $Eu_2O_3$ was investigated. The compacts were made by cold pressing, at 10 000 psi, $Eu_2O_3$ powder that previously had been heated to 1700°C in hydrogen for 3 hr and then sintering to 1230°C for 1 hr in hydrogen. Each compact represented a separate batch of europia. None of the compacts showed any apparent reaction after 18 hr in $H_2O$ at 25°C, but all suffered fairly rapid decomposition in boiling water. After 2 hr at 100°C, all pellets showed evidence of attack, and the pellet from so-called "Jar-7" material (a reference oxide notable for having been satisfactorily incorporated into absorber plates) was completely decomposed. After an additional 3 hr, another pellet was completely decomposed, and the other three samples showed extensive attack. After cooling and standing overnight in room-temperature water, these pellets appeared swollen and were too weak to handle with forceps. It was observed that those compacts which were dark gray in appearance decomposed more slowly than the lighter colored compacts, but no explanation for this difference can be advanced at this time. X-ray diffraction analysis of powder taken from each of the compacts after the water corrosion experiment showed that a second phase, tentatively identified as $Eu(OH)_3$, was present in addition to monoclinic $Eu_2O_3$. Although no data are available for the x-ray diffraction pattern of $Eu(OH)_3$, it was possible to index seven lines from the pattern of the second phase by assuming it would be similar to $La(OH)_3$, which is hexagonal and isostructural with $Sm(OH)_3$ and $Gd(OH)_3$. It was observed that the intensity of the $Eu(OH)_3$ diffraction pattern was strongest in the residue from the compact which first decomposed in boiling water. Apparently, the aqueous corrosion resistance of $Eu_2O_3$ compacts is related to resistance of the material to hydrolysis.

## Stability of Europium Oxide in Silicon-Bearing Stainless Steel

C. F. Leitten, Jr.

The stability of $Eu_2O_3$ dispersed in silicon-bearing stainless steel powder compacts was studied[2] in the temperature range 900 to 1250°C. The effects of silicon content of the stainless steel powder, oxide-conditioning treatment, and heat-treating time and atmosphere were also investigated.

Independent of the conditioning process employed, $Eu_2O_3$ reacted with the austenitic stainless steel, as manifested by compact volume increases and the deposition of an europium-bearing, yellow-green film on the specimen surfaces. The degree of reaction was observed to increase with increasing silicon content in the steel. Volume increases of approximately 6% were noted in stainless steel-base compacts containing 2 wt % Si when heat treated at 1230°C for 1 1/2 hr. The presence of a reaction product was also observed in the $Eu_2O_3$ particles in the high-silicon-bearing stainless steel compacts as a result of reaction. Stainless steel-base dispersions containing 0.11 wt % Si showed slight volume decreases on heat treating; however, the deposition of the reaction film was also noted on these specimen surfaces. The presence of a reaction product in the oxide particles was not observed in these compacts.

Elemental iron, nickel, and chromium with silicon content less than 58 ppm were stable with $Eu_2O_3$ at a temperature of 1230°C. Depending on the oxygen content of the chromium, slight interactions of $Eu_2O_3$ and chromium oxide were noted at the particle interfaces. The instability noted between $Eu_2O_3$ and chromium containing 0.12 wt % Si was manifested by a volume increase and the deposition of the yellow-green reaction film. No reaction product, however, was noted in the europium oxide particles.

The heat-treating atmosphere did not appear to affect the presence of the reaction in the investigated material combinations but did affect the degree of reaction. Specimens heat treated in hydrogen appeared to have larger volume growths than compacts heat treated in helium or vacuum. The degree of reaction was observed to increase with time and temperature, independent of the atmosphere.

Efforts to establish basic standards for identification of the various reaction products involved studies of the europium-silicon alloy system and of $Eu_2O_3$ dispersions in silicon and $SiO_2$. The reaction of $Eu_2O_3$ with silicon and with $SiO_2$ at 1200°C generally resulted in compact volume increases and the deposition of the yellow-green film on the specimen surfaces. The formation of $EuSi_2$ was positively established as a reaction product in the silicon-base compacts. Few difficulties were encountered in preparing the various europium-silicon alloys by arc melting, other than a considerable loss of europium, which was noted in each alloy, as a result of vaporization. A preliminary study was made on these alloys in the composition range 9 to 91% Eu. The possible existence of at least three silicides was noted by examination of x-ray diffraction patterns. The cast microstructure of alloys between 9 and 63 wt % Eu consisted of silicon and $EuSi_2$.

## Boron-Gradient Neutron Absorbers

R. J. Beaver T. D. Watts

Irradiation test data obtained on 3 wt % dispersions of boron in iron have shown that it may be possible for such material to withstand as much as 7 at. % burnup of $B^{10}$ atoms without significant damage. Microstructural examination of the irradiated specimens has revealed that, because of the self-shielding, boron in surface layers of the dispersion is burned to appreciably higher values than in the underlying material.[6] For example, in undamaged specimens which were subjected to an average $B^{10}$ burnup of 4 at. %, the $B^{10}$ burnup at the surface was as high as 30 at. %. Specimens exposed to an average burnup of 11 at. % had a surface burnup of 70 at. %, and severe damage in the surface layers was observed. It may be possible to circumvent this problem by designing the absorber so that the $B^{10}$ burnup will be uniform throughout the thickness. As shown in Fig. 4.1, the boron distribution increases from the surface of the neutron absorber plate

[6] C. F. Leitten, Jr., et al., J. Nuclear Materials, 2: 136–44 (1959).

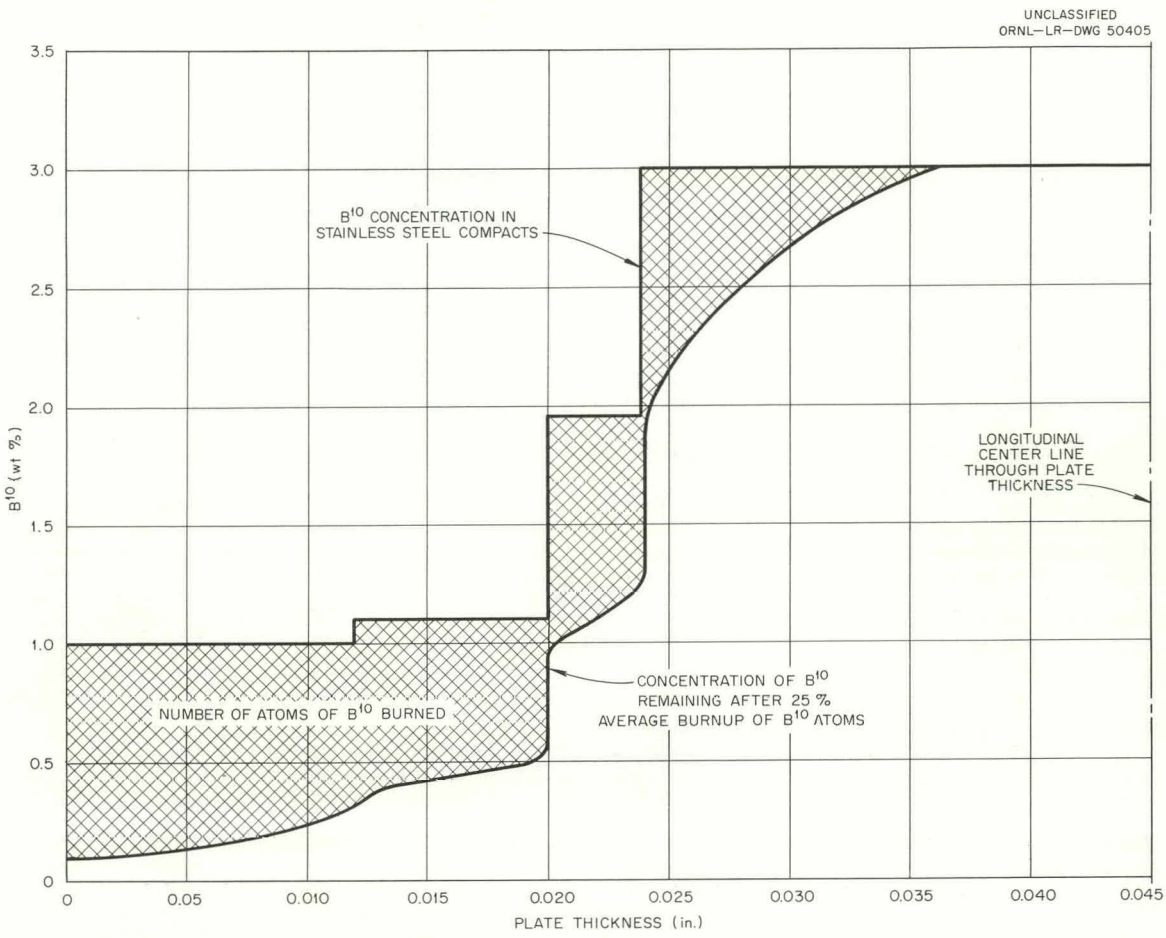


Fig. 4.1. Profile of Boron Concentration Gradient and $B^{10}$ Burnup Limits in Half Thickness of an SM-1 Reactor Neutron Absorber Plate Designed to Obtain an Average Burnup of 25% of $B^{10}$ Atoms with No Significant Damage. Other half thickness is symmetrical with the section illustrated.

to the interior in step-wise fashion. The data of Fig. 4.1 illustrate a conservative design based on 3 wt % B–Fe specimens, which showed that this material can successfully withstand a burnup of $4.7 \times 10^{21}$ atoms of $B^{10}$ per cubic centimeter of material. This particular gradient is based on the assumption that an average burnup of 25 at. % $B^{10}$ can be obtained without significant damage. It is anticipated that the test section will not become damaged through one core life in the SM-1 reactor.

A full-size neutron absorber section has been prepared for irradiation testing in the SM-1 reactor. The purpose of this test is to demonstrate the reliability of the boron-gradient concept. The over-all design of the section is similar to the design of the neutron absorbers presently

operating in the SM-1 reactor, except the core section of the composite fuel plate contains the boron gradient described above. The boron is 92% enriched in the $B^{10}$ isotope and is dispersed in type 200 stainless steel by conventional powder-metallurgy methods. Fabrication studies indicated that the most compatible sintering temperature was 1050°C. With this exception, the procedures used to make the powdered compacts and fabricate composite plates were identical with those previously reported for manufacturing the europium-bearing absorber sections.[3]

As part of the fabrication development for this component, an evaluation was conducted to determine whether boron losses or significant interdiffusion of boron occurred as a result of rolling at a temperature of 1150°C and subsequently annealing at 1000°C. From the data presented in Table 4.3, it may be concluded that slight interdiffusion occurred, but the losses were not important. A hardness traverse was also made across the gradient. The results are presented in Fig. 4.2, which metallographically depicts the boron gradient in the as-polished condition. As expected, the hardness values correlate well with the boron concentration; that is, 257 DPH for a concentration of 1.14 wt % B and 348 DPH for the stainless steel containing 3.44 wt % B.

The absorber box was welded with no difficulty. It successfully passed a reactivity measurement in the Alco Products Critical Test Facility and is presently under test in the SM-1 reactor. Pertinent details of the boron content are listed in Table 4.4, and the critical dimensional measurements are illustrated in Fig. 4.3.

Table 4.3. Boron Analysis of Fabricated Gradient Plate

| Layer No. | Charged Boron (wt %) | Analyzed Boron[a] (wt %) |
|---|---|---|
| 1 | 1.20 | 1.18 |
| 2 | 1.34 | 1.57 |
| 3 | 2.51 | 2.86 |
| 4 | 3.76 | 3.48 |

[a]The results show some leveling off of the section due to interdiffusion.

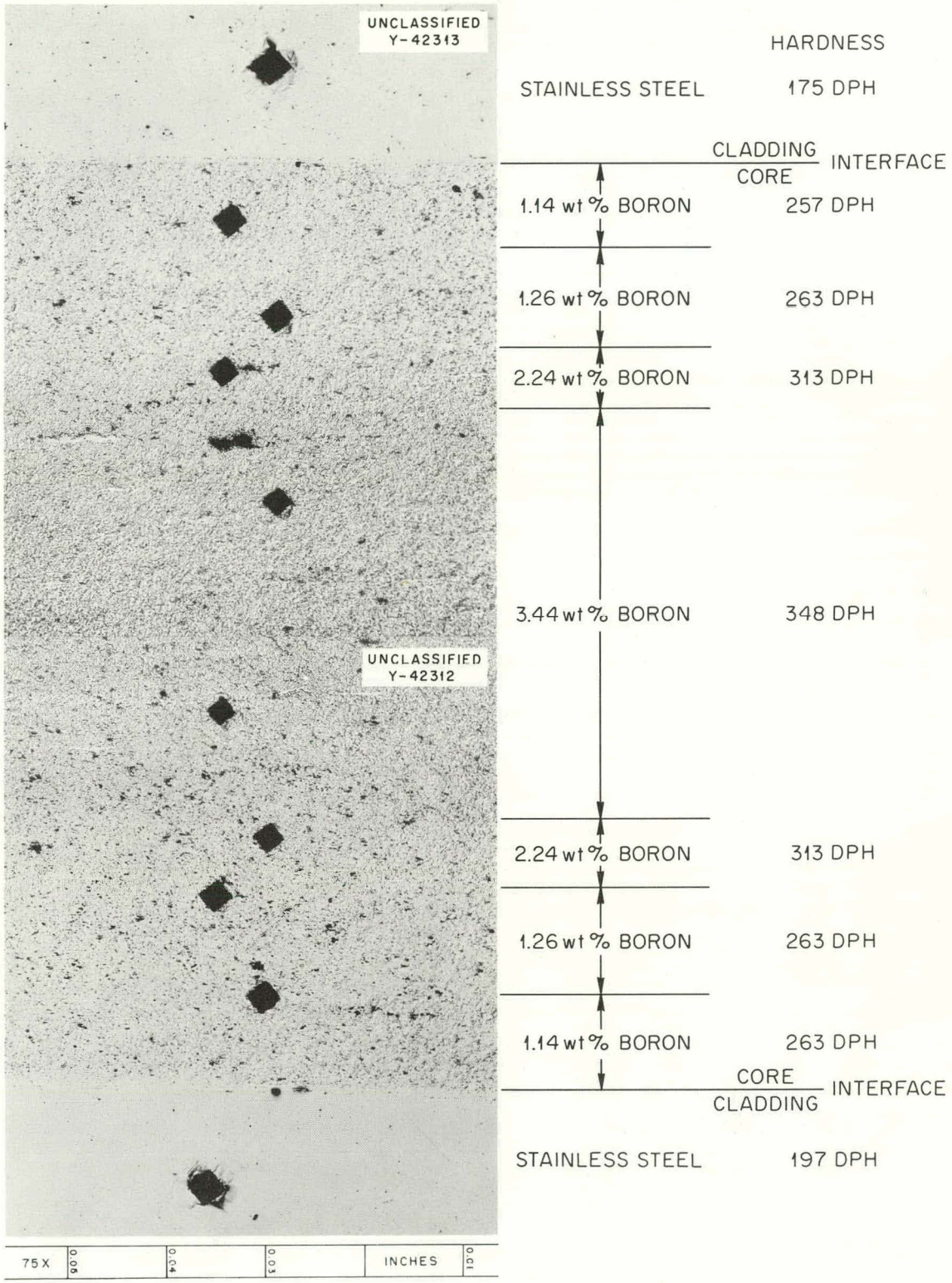


Fig. 4.2. Transverse Section of Boron Gradient Plate Showing Effect of Boron Concentration in Austenitic Stainless Steel on Hardness Values. As polished. 75X (Original reduced 19%)

Table 4.4. Data on Boron Gradient Absorber Section Under Test in SM-1 Reactor

Identification number: BG-1
Number of cores per plate: 8

| Type | Core Makeup | | |
|---|---|---|---|
| | Boron[a] (g) | Stainless[b] Steel (g) | Boron Concentration (wt %) |
| 1 | 0.70 | 61.42 | 1.14 |
| 2 | 0.52 | 41.91 | 1.26 |
| 3 | 0.47 | 18.73 | 2.24 |
| 4 | 3.48 | 97.34 | 3.44 |
| 4 | 3.48 | 97.34 | 3.44 |
| 3 | 0.47 | 18.73 | 2.24 |
| 2 | 0.52 | 41.91 | 1.26 |
| 1 | 0.70 | 61.42 | 1.14 |
| Total | 10.34[c] | 438.80[c] | |

[a] 92% enriched in the $B^{10}$ isotope.

[b] Nominal composition: 0.03% C, 20.70% Mn, 16.37% Cr, 0.49% Ni, balance Fe.

[c] Loading per plate.

## Boron-Gradient Control Rod with a Tip End Containing $Eu_2O_3$ in Stainless Steel

R. J. Beaver T. D. Watts

An effort has been made to reduce the cost of the previously developed $Eu_2O_3$-stainless steel neutron absorber section by limiting the irradiation-resistant but high-cost europium oxide to the tip end (6 1/2 in.) of the 20 5/8-in.-long absorber section. The balance of each absorber plate contains a boron gradient of the type described in the previous section. Thus, material cost, as reflected by the price of europium oxide, is significantly reduced, and yet it is felt that the life of the absorber will not be impaired, since only the tip end is burned out to any great extent. The conceptual design of this type of plate is shown in Figs. 4.4 and 4.5.

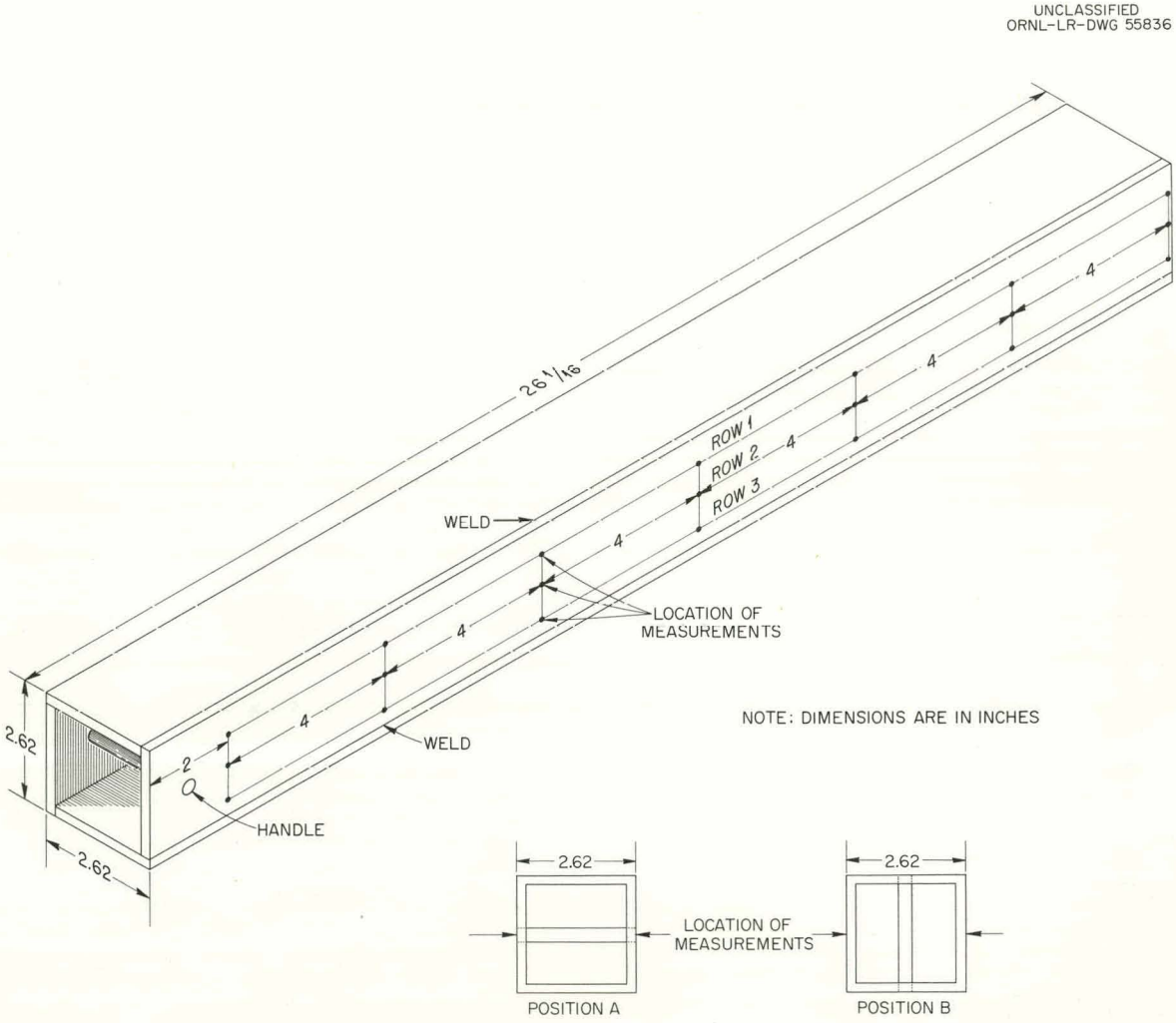


Fig. 4.3. Locations of Dimensional Measurements of Welded BG-1 Neutron Absorber Section for SM-1 Test.

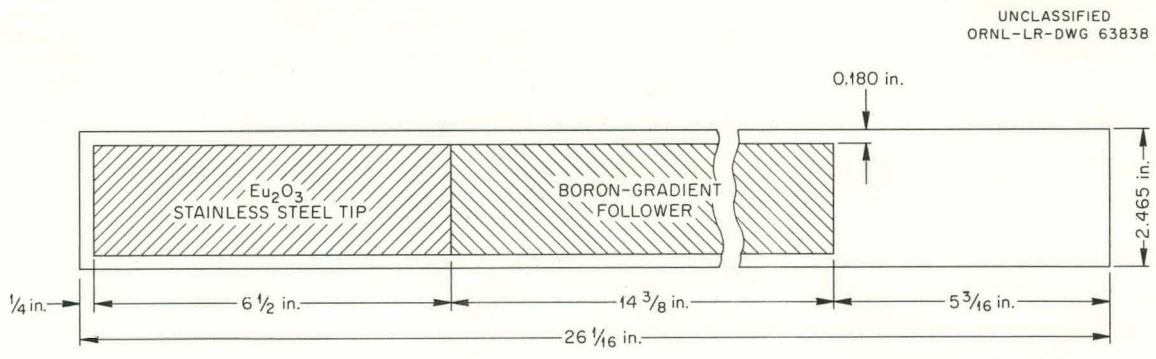


Fig. 4.4. Plan View Showing Design of $Eu_2O_3$-Stainless Steel Tip and Boron Gradient Follower in SM-1 Reactor Neutron Absorber Plate.

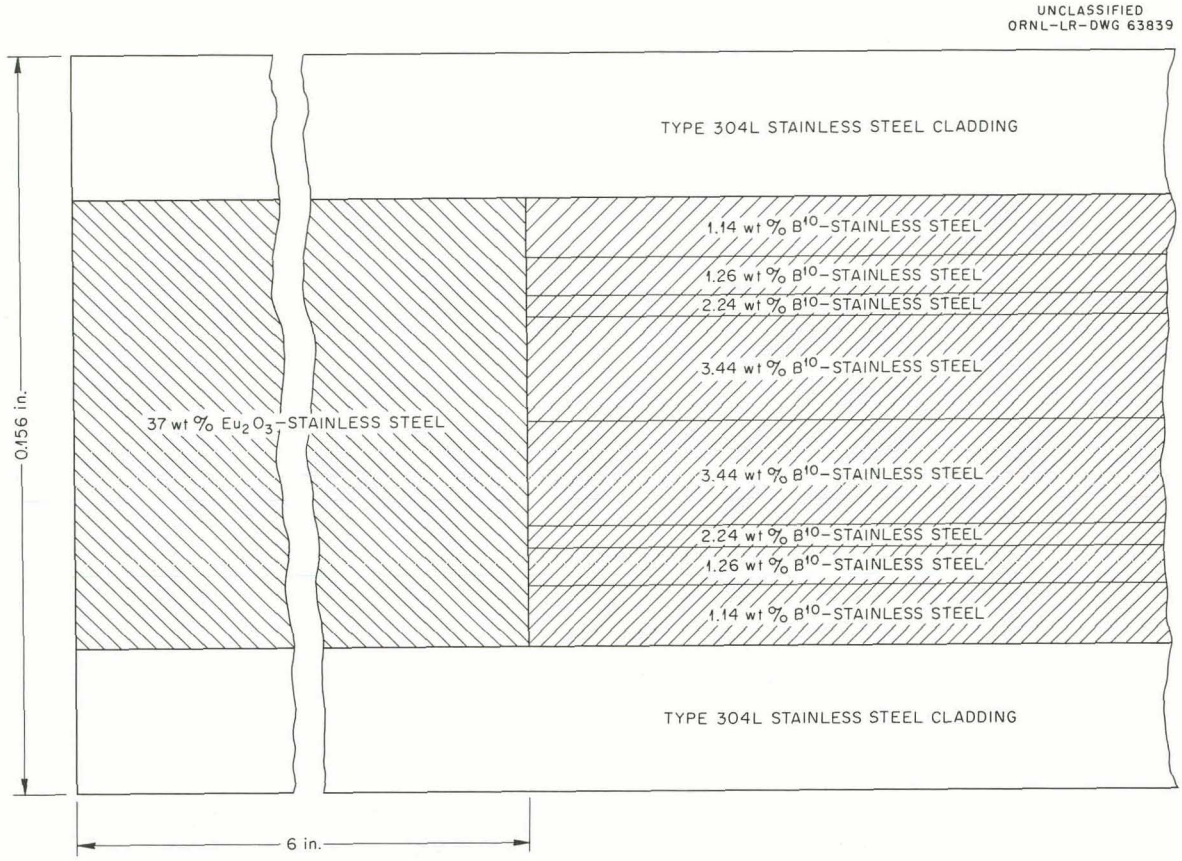


Fig. 4.5. Longitudinal Section of Composite Plate Showing Arrangement of $Eu_2O_3$-Stainless Steel Tip with Boron Gradient Follower.

Full-size sample plates have been prepared from 37 wt % $Eu_2O_3$–elemental stainless steel compacts prepared by established techniques[3] and boron-gradient compacts prepared in the manner previously described. Radiographic examination of the plates showed them to be dimensionally acceptable for irradiation testing in the SM-1 reactor.

Metallographic observations revealed considerable intermixing of the boron dispersion with the $Eu_2O_3$ dispersion at the junction of these two materials. Because of this mixing, the silicon-bearing stainless steel matrix of the boron region is in intimate contact with $Eu_2O_3$. Thus, a condition is created for reaction of $Eu_2O_3$ with silicon.[2] The mixing is illustrated in Figs. 4.6 and 4.7. There is some indication of a slight

reaction of the europium oxide with the type 200 stainless steel used as the matrix in the gradient region. This is evidenced by the darker appearance of $Eu_2O_3$ particles adjacent to the interface between the tip and the body of the plate. This slight reaction is not felt to be harmful. Fabrication of a full-size component for testing in the SM-1 reactor is in progress.

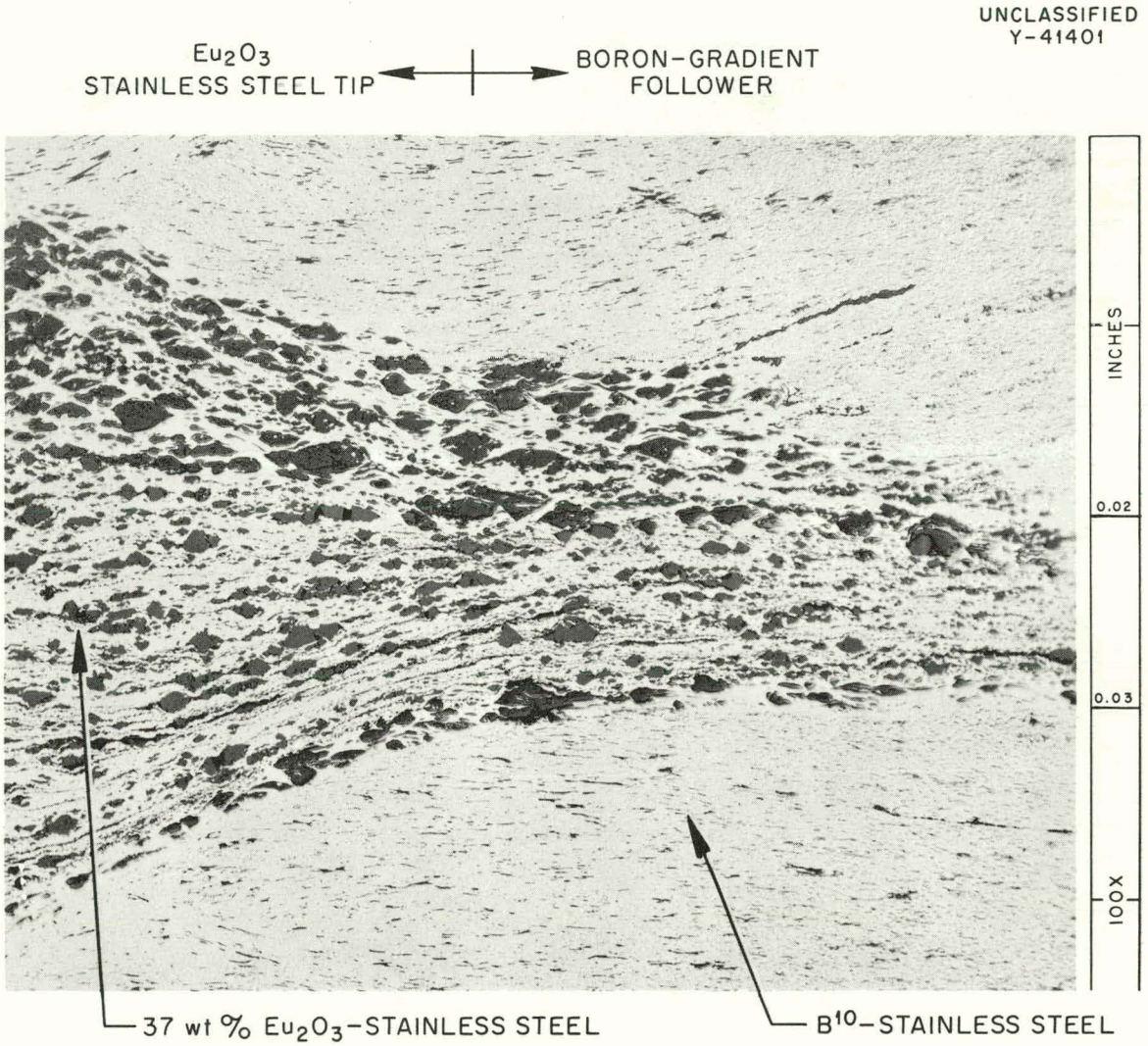


Fig. 4.6. Longitudinal Section of $Eu_2O_3$-Tip Neutron-Absorber Plate Showing Mixing of the $B^{10}$-Stainless Steel Dispersion with the Dispersion of 37 wt % $Eu_2O_3$–Stainless Steel at the Junction of These Two Materials. As polished. 100X

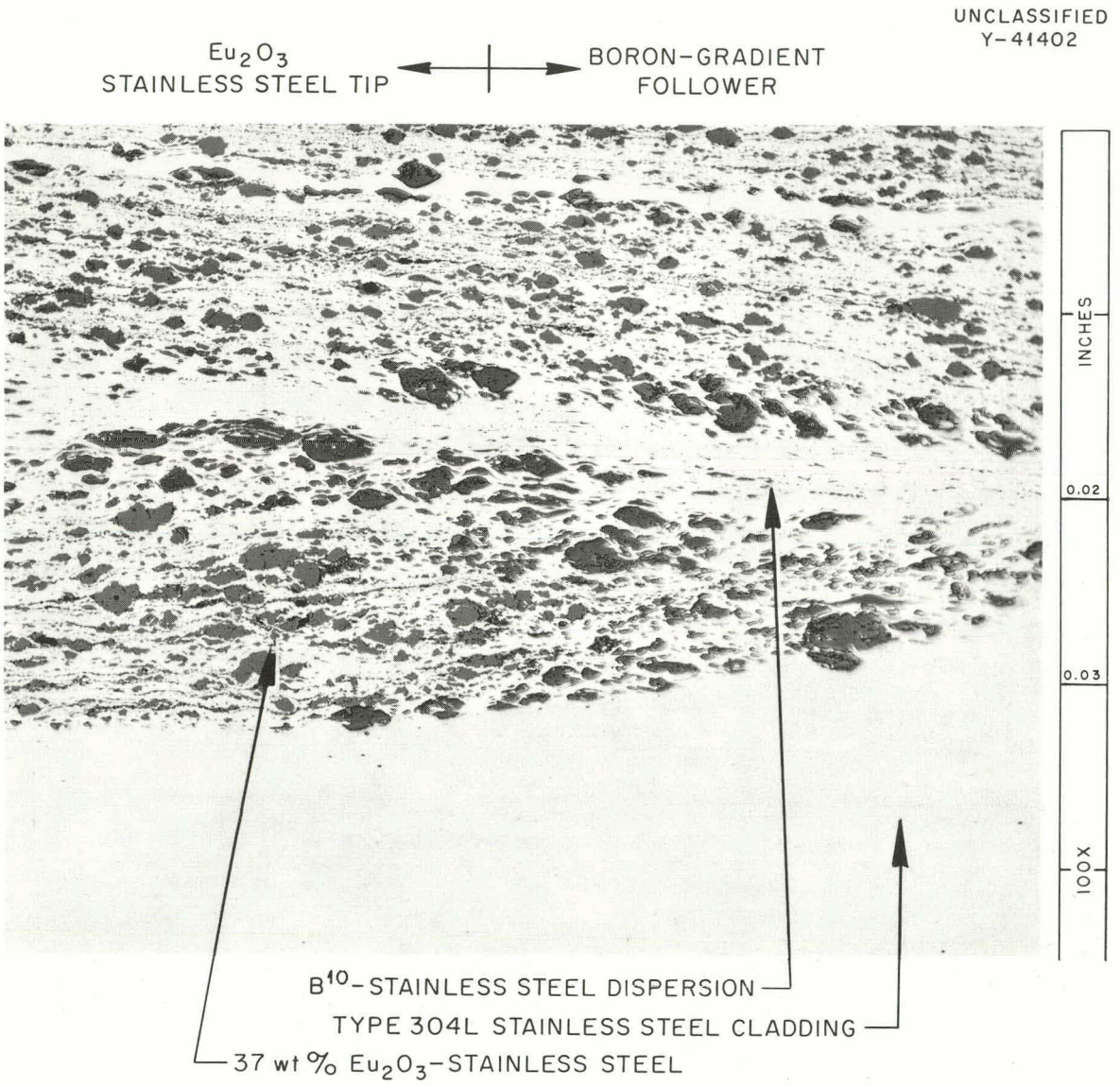


Fig. 4.7. Longitudinal Section a Short Distance from the Junction of the Dispersion of 37 wt % $Eu_2O_3$–Stainless Steel and the $B^{10}$-Stainless Steel Mixture Showing the Intermingling of These Materials. As polished. 100X.

## 5. IRRADIATION TESTING OF FUEL AND ABSORBER MATERIALS

### Postirradiation Examination of SM-1 Fuel Elements

A. E. Richt

The effects of irradiation on fuel elements that have been removed from the active lattice of the SM-1 reactor are being studied. The fuel element consists of 18 composite fuel plates joined by brazing into a pair of side plates to form an integral assembly. The flat, rectangular plate is composed of a 0.020-in.-thick core section containing 25 wt % $UO_2$ and 0.13 wt % $B_4C$ in a matrix of type 302B stainless steel. The fuel section is clad with 0.005 in. of type 304L stainless steel by roll bonding.[1]

Results of postirradiation examination of the first stationary fuel element (S-72), which was removed after 10.5 Mwyr of operation, were reported previously.[2] No dimensional changes of significance occurred, although rippling of the outer fuel plates in the assembly was observed. Examination of the Coast Metals N.P. brazed joints revealed significant localized attack by the reactor coolant water. Very infrequent intergranular cracking in the stainless steel cladding was also noted. Measured burnup in terms of per cent $U^{235}$ depletion was 16% (average) and 38% (maximum).[3]

Postirradiation examination of a second stationary fuel element (S-79) is now essentially complete. This element operated for 16.4 Mwyr in the SM-1 reactor, and measured burnup values indicate average and maximum $U^{235}$ atom depletions of 42 and 57%, respectively. The peak fission burnup expressed as fissions per cubic centimeter was $22.5 \times 10^{20}$.

Over-all dimensional measurements of this fuel element did not show any changes of significance. However, examination of the contour of the

---

[1]J. E. Cunningham et al., Specifications and Fabrication Procedures for APPR-1 Core II Stationary Fuel Elements, ORNL-2649, Jan. 29, 1959.

[2]APPR Ann. Prog. Rep. Jan. 31, 1960, ORNL-2907, p. 32.

[3]Met. Div. Ann. Prog. Rep. July 1, 1960, ORNL-2988, p. 311.

outer plates revealed a larger magnitude of rippling than in the element, S-72. The effect is illustrated in Fig. 5.1. Measurements of spacing between plates 1 and 2 demonstrated the influence of rippling in the first plate on the underlying spacing. This effect is shown graphically in Fig. 5.2, which also shows the measurements of the spacings between plates 9 and 10, which are near the midplane of the fuel element. As reported previously for fuel element S-72, the inner plate spacings did not change significantly, indicating that rippling of the inner fuel plates is probably negligible.

Metallographic examination of the fuel matrix failed to reveal any cracking or other gross deterioration. As expected, considerable porosity,

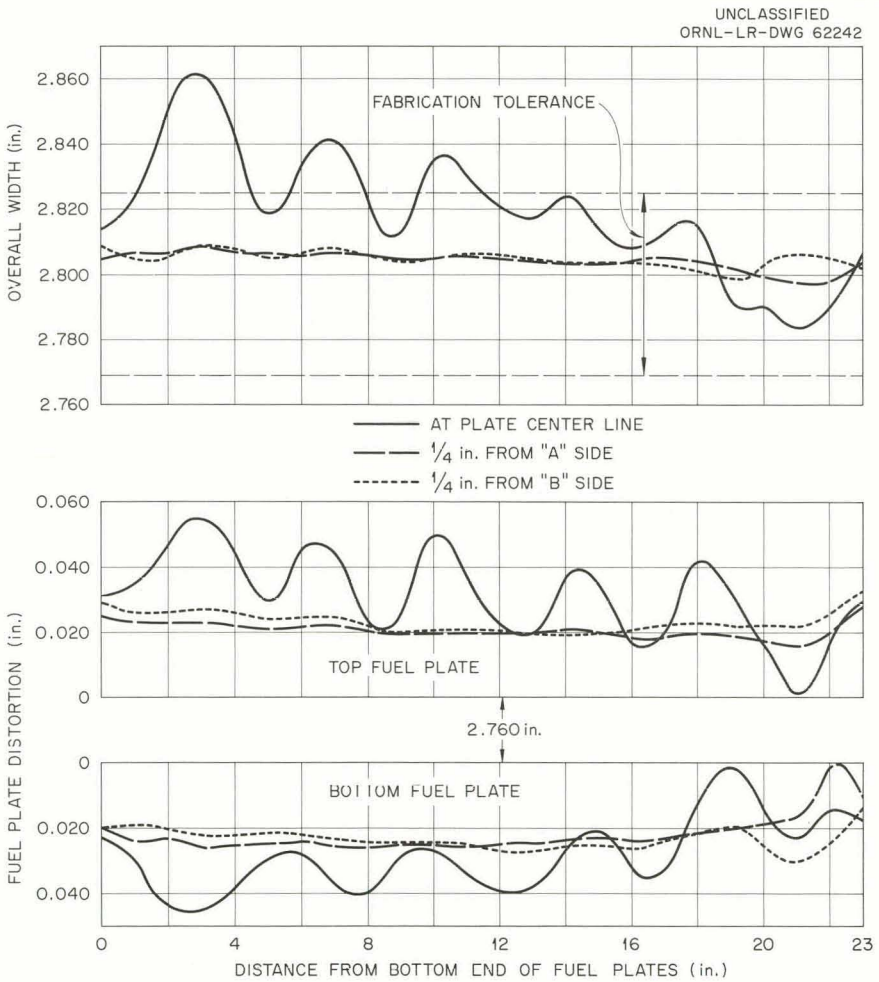


Fig. 5.1. Dimensional Profiles Across Fuel Plates of Fuel Element S-79.

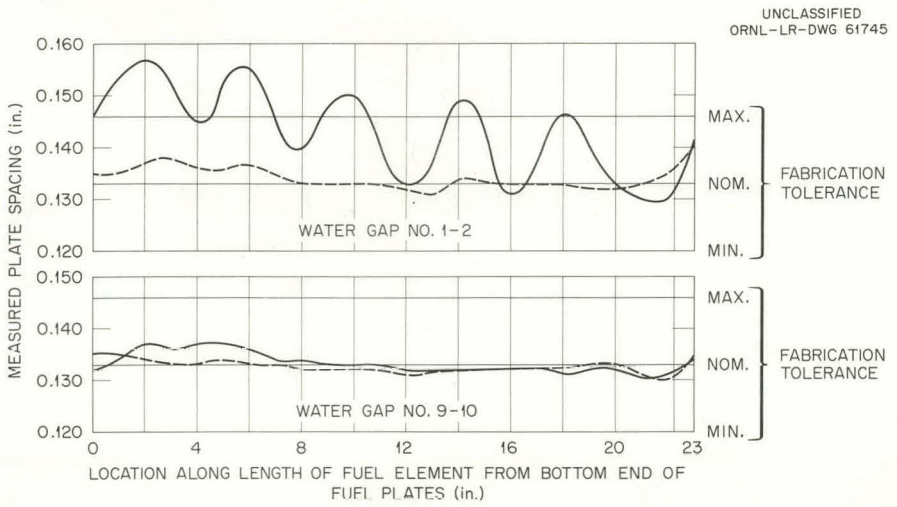


Fig. 5.2. Plate Spacing Measurements of SM-1 Fuel Element S-79.

attributable to fission-gas precipitation, was found in the $UO_2$. In addition, the presence of two unidentified phases was noted. An effort is being made to identify these phases. These microstructural effects are illustrated in Fig. 5.3.

As shown in Fig. 5.4, the Coast Metals N.P. joint was severely corroded by the pressurized-water environment. Corrosion appeared to be confined to the brittle eutectic mixture in the braze metal fillet. A comparison with the corrosion of joints in fuel element S-72 indicated that the longer in-pile exposure of fuel element S-79 had not significantly increased the degradation of the brazed joints.

The rather severe corrosion to these joints was surprising in view of out-of-pile corrosion tests conducted on this alloy.[4] It is postulated that the deterioration shown may be due to the generation of cracks in this alloy by stresses induced during reactor operation. Cracking would be followed by an acceleration of attack from a crevice corrosion process.

As illustrated in Figs. 5.5 and 5.6, both intergranular and transgranular cracking of the 0.005-in.-thick type 304L stainless steel cladding were observed in element S-79. Only a very few intergranular cracks in the cladding had been noted previously in fuel element S-72. Although

---

[4]R. J. Beaver et al., An Investigation of the Corrosion Resistance of Brazing Alloys for Austenitic Stainless Steel Fuel Elements in 565°F Pressurized Water, ORNL-2834 (in press).

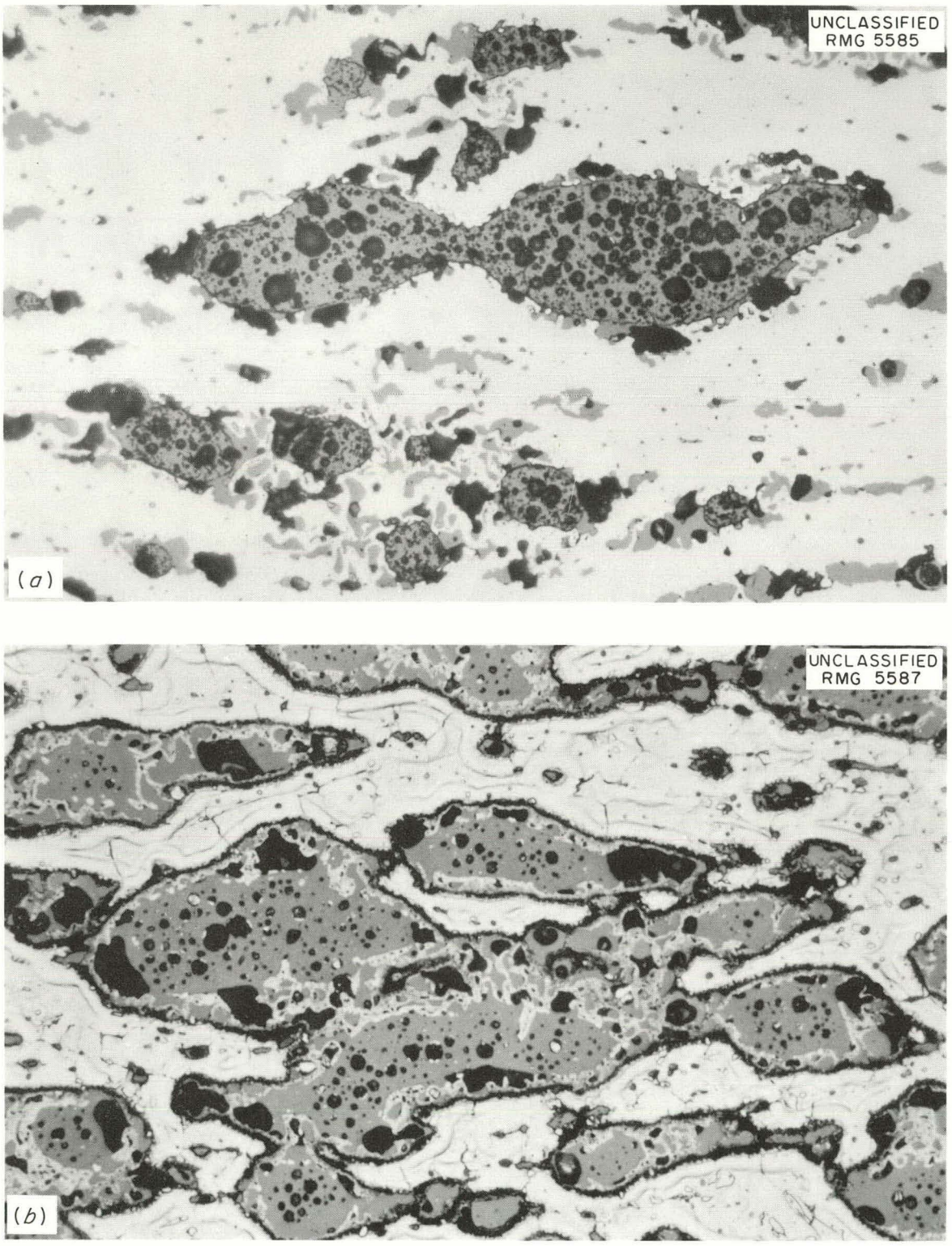


Fig. 5.3. Typical Microstructures of SM-1 Fuel Plate After 47% Fission Burnup of $U^{235}$ ($22.5 \times 10^{20}$ Fissions/$cm^3$). (a) Etched with $H_2SO_4$-$H_2O_2$-$H_2O$. (b) Etched with glycerol regia. 500X

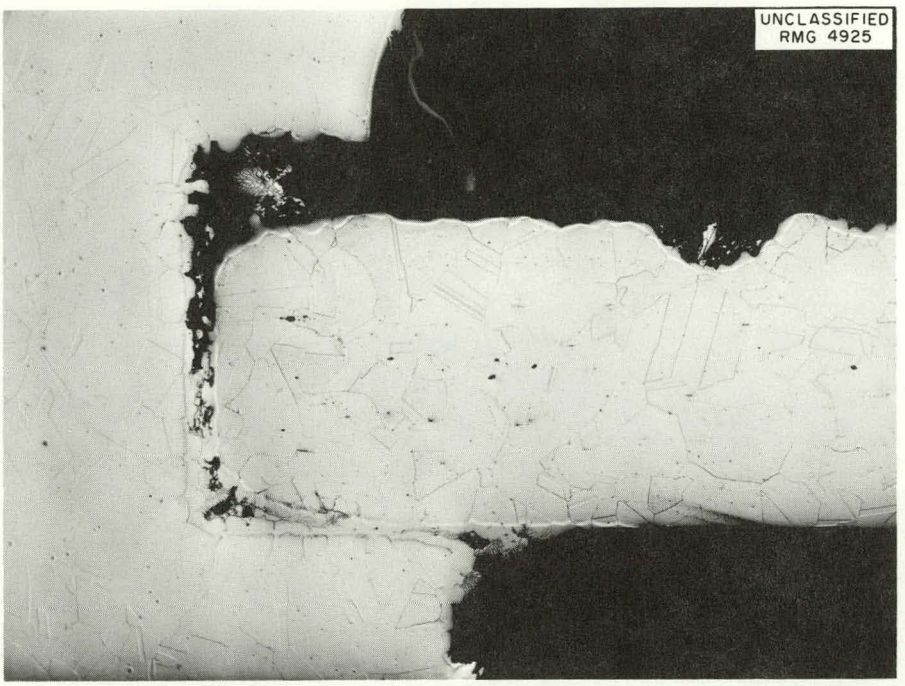


Fig. 5.4. Typical Microstructure of Fuel Plate to Side Plate Brazed Joint Showing Corrosion of Eutectic Mixture. Specimen was in the SM-1 reactor about three years. Etchant: glycerol regia. 75X (Original reduced 23%)

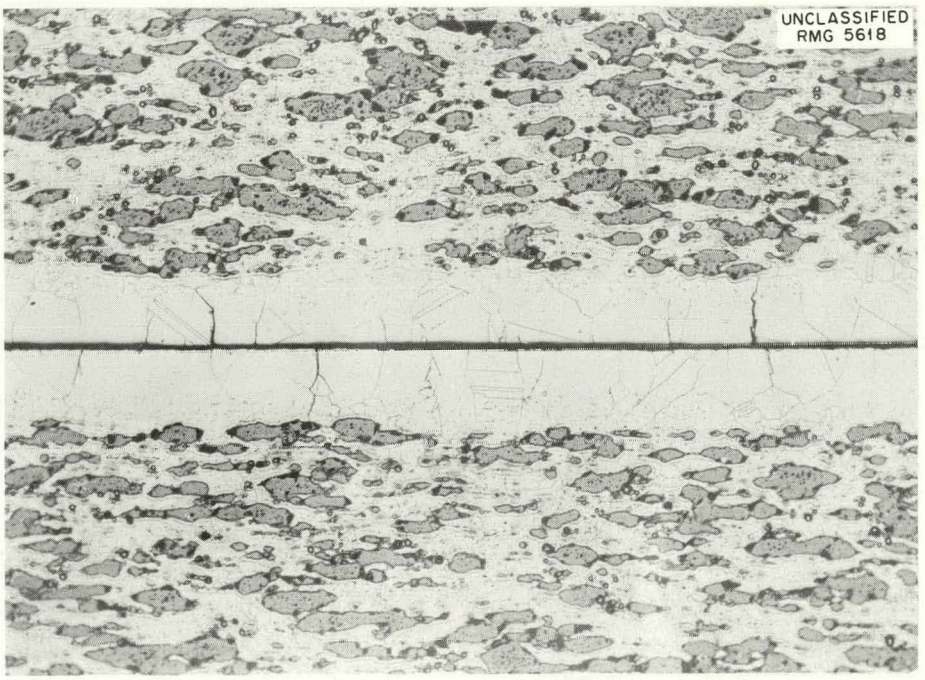


Fig. 5.5. Cracking of Fuel Plate Cladding in SM-1 Fuel Element S-79. Etchant: glycerol regia. 100X (Original reduced 21%)

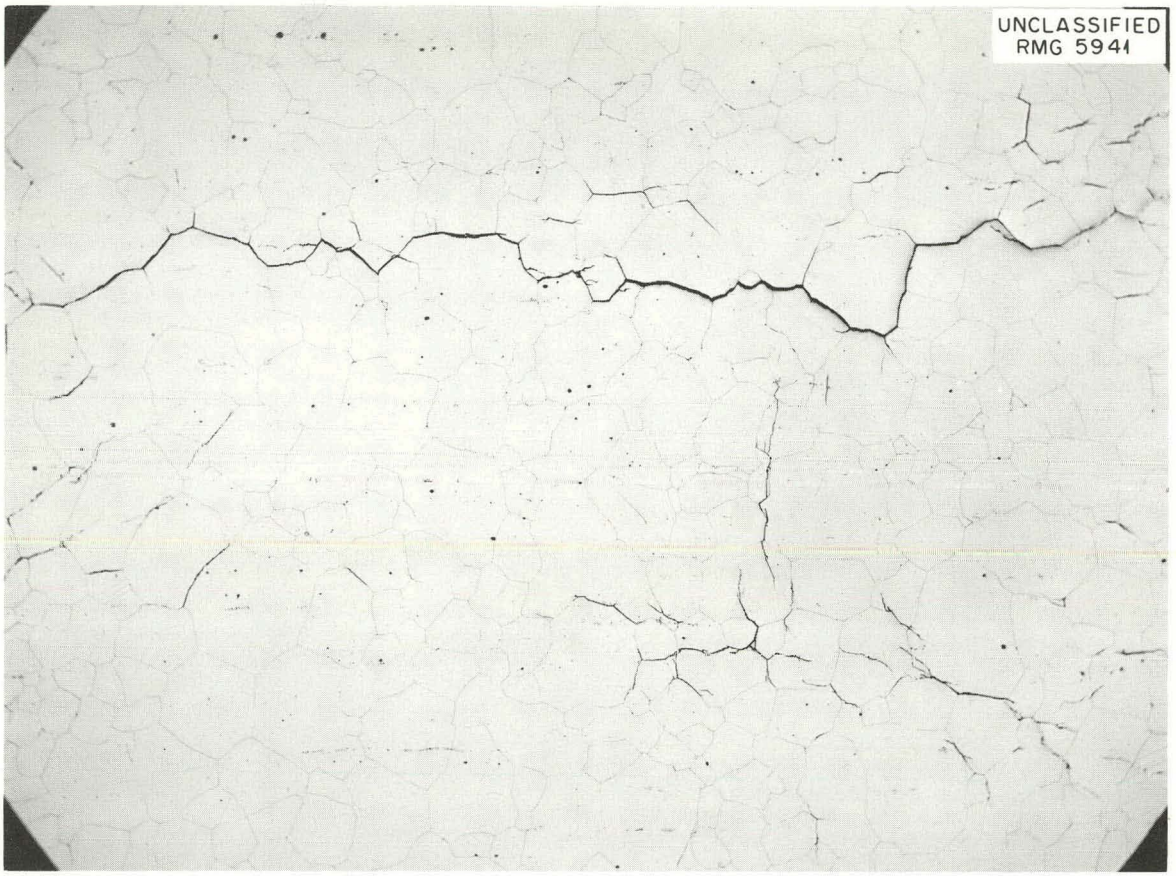


Fig. 5.6. Cracking Patterns in Fuel Plate Cladding. View shown is a polished and etched fuel plate surface. Etchant: glycerol regia. 75X

some cracks penetrating to the surface of the fuel section can be seen, no penetrations into the matrix were found. The cause for the intergranular cracking may be related to the fact that the fabrication process results in carburization of the type 304L stainless steel cladding and ultimately the material becomes sensitized as well as very coarse grained.[5] The cause for the transgranular cracking may be due to a stress-corrosion phenomenon, although it is not obvious why it was not observed in the previously examined fuel element.

---

[5]R. J. Beaver et al., Investigation of the Factors Affecting Sensitization of Army Package Power Reactor (APPR-1) Fuel Elements, ORNL-2312, Sept. 18, 1957.

## Postirradiation Examination of Neutron Absorbers Containing 3 wt % Boron in Iron

A. E. Richt

The first neutron-absorber section for the SM-1 control rod consisted of stainless steel-clad plates containing 3 wt % B in iron.[6] The boron used was 90% enriched in the $B^{10}$ isotope. At the time of this development, an irradiation testing program was initiated at the MTR on miniature versions of these composite plates.[7] Although the irradiation testing temperature was only 150°F, it was assumed that postirradiation heat treatments at 600°F would more than adequately simulate the 500°F surface temperature of the neutron-absorber plates in the SM-1 plant. Initial results[8] from this program indicated that early failure was likely to occur in the full-size neutron absorbers in the SM-1. Examination of two of these full-size rods exposed in the SM-1 reactor for two-thirds of the core life supported these findings, and the iron-boron neutron absorbers were replaced with absorbers containing 37 wt % $Eu_2O_3$ in stainless steel.

The final phase of the MTR irradiation testing program has been completed and the results are summarized in Fig. 5.7. These data show thickness increases of the miniature composite plates as a function of $B^{10}$ burnup after irradiation at 150°F. No other dimensional changes occurred. As reported previously, significant changes in thickness were a result of failure at the core-to-cladding interface.[8] Helium pressure is no doubt responsible for the failures.

The summary in Fig. 5.7 shows that specimens with 5% burnup of $B^{10}$ atoms did not exhibit significant increases in thickness. Metallographic examination revealed that the core-to-cladding interface was still intact. At burnups of 11% and greater, failures at the core-to-cladding interface occurred and all specimens exhibited significant thickness increases.

---

[6] R. J. Beaver et al., Specifications for Army Package Power Reactor (APPR-1) Fuel and Control Rod Components, ORNL-2225, July 24, 1957.

[7] C. F. Leitten, Jr., Phase III Absorber Rod Sample Irradiation — Irradiation Request ORNL-MTR-28, ORNL CF-57-7-19, July 5, 1957.

[8] C. F. Leitten, Jr., et al., J. Nuclear Materials, 2: 136–44 (1959).

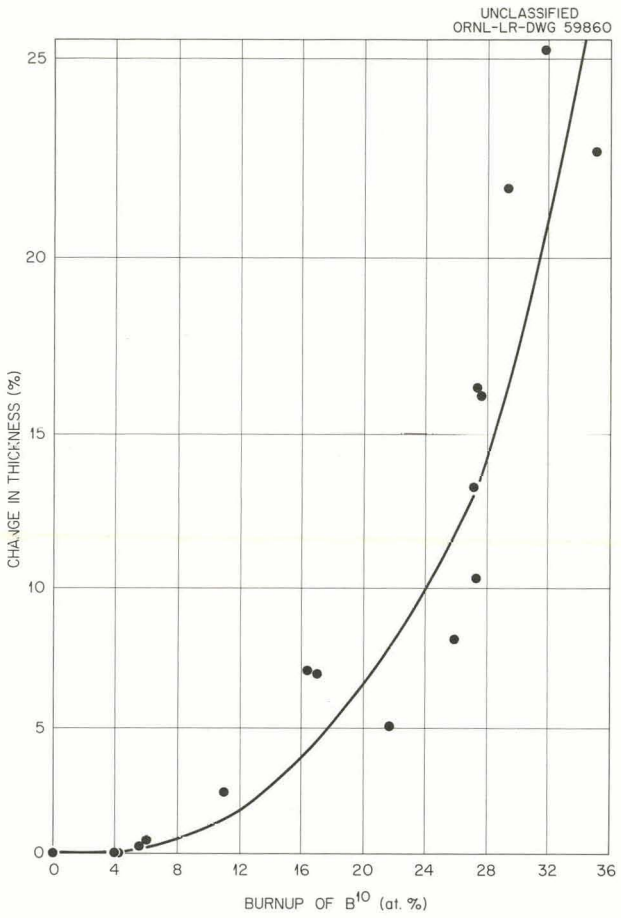


Fig. 5.7. Effect of Burnup on Swelling of Fe-$B^{10}$ Miniature Absorber Plates at a Temperature of Approximately 130°F.

Since no data exist in the range of 7 to 10% burnup, it is not possible to establish the exact burnup at which failure by separation at the core-to-cladding interface occurs.

All specimens exhibiting failures at the core-to-cladding interface after irradiation showed additional increases in thickness when heat treated at 600°F. Those with bonding still intact were unaffected by the heat treatment. The results shown in Fig. 5.7 are in general agreement with data previously reported on the full-size absorber sections which were removed from the first core of the SM-1 reactor.[2]

## Irradiation Testing and Postirradiation Examination of Dispersions of $Eu_2O_3$ in Stainless Steel Irradiated at 150°F

A. E. Richt

The neutron-absorber boxes presently operating in the SM-1 reactor are composed of stainless steel-clad plates containing a dispersion of 37 wt % $Eu_2O_3$ in stainless steel.[9] During the development of this type of dispersion, an irradiation program[10] was initiated to test miniaturized composite plates in the ETR at a temperature of approximately 150°F. Specimens submitted for testing contained 20, 30, and 40 wt % $Eu_2O_3$ dispersed in stainless steel. Several of these specimens were examined after irradiation to the exposures listed in Table 5.1. Dimensional measurements of the specimens and metallographic examination of the matrix material did not reveal any loss of structural integrity. No dimensional

Table 5.1. Irradiation History of $Eu_2O_3$-Bearing Miniature Absorber Plates

| Specimen No. | Core Loading (wt % $Eu_2O_3$) | Integrated Flux[a] (neutrons/$cm^2$) |
|---|---|---|
| | | $\times 10^{20}$ |
| 39-1 | 20 | 7.0 |
| 39-2 | 20 | 12.1 |
| 39-5 | 30 | 7.6 |
| 39-6 | 30 | 14.6 |
| 39-9 | 40 | 7.2 |
| 39-10 | 40 | 14.8 |

[a]Unperturbed; from ETR estimates.

changes were noted and the irradiated microstructure was indistinguishable from the as-fabricated structure.

---

[9]C. F. Leitten, Jr., et al., Specifications and Fabrication Procedures in Europium-Bearing Absorber Rods for Reactivity Control in Core II of SM-1, ORNL-2733, July 29, 1959.

[10]C. F. Leitten, Jr., The Irradiation of Miniature $Eu_2O_3$-Bearing Absorber Plates — Irradiation Request ORNL-MTR-39, ORNL CF-59-9-25, Sept. 14, 1959.

Postirradiation studies were conducted to determine the corrosion behavior of intentionally defective samples after irradiation. These tests were run in static autoclaves in 300°C water pressurized at 1200 psi. Specimens placed in these tests had edges sheared to expose the $Eu_2O_3$-stainless steel material to the aqueous environment. The results of tests on the irradiated specimens are compared with the unirradiated material, similarly exposed, in Fig. 5.8 and Table 5.2. As shown in Fig. 5.8, exposure of the irradiated material to this environment has resulted in

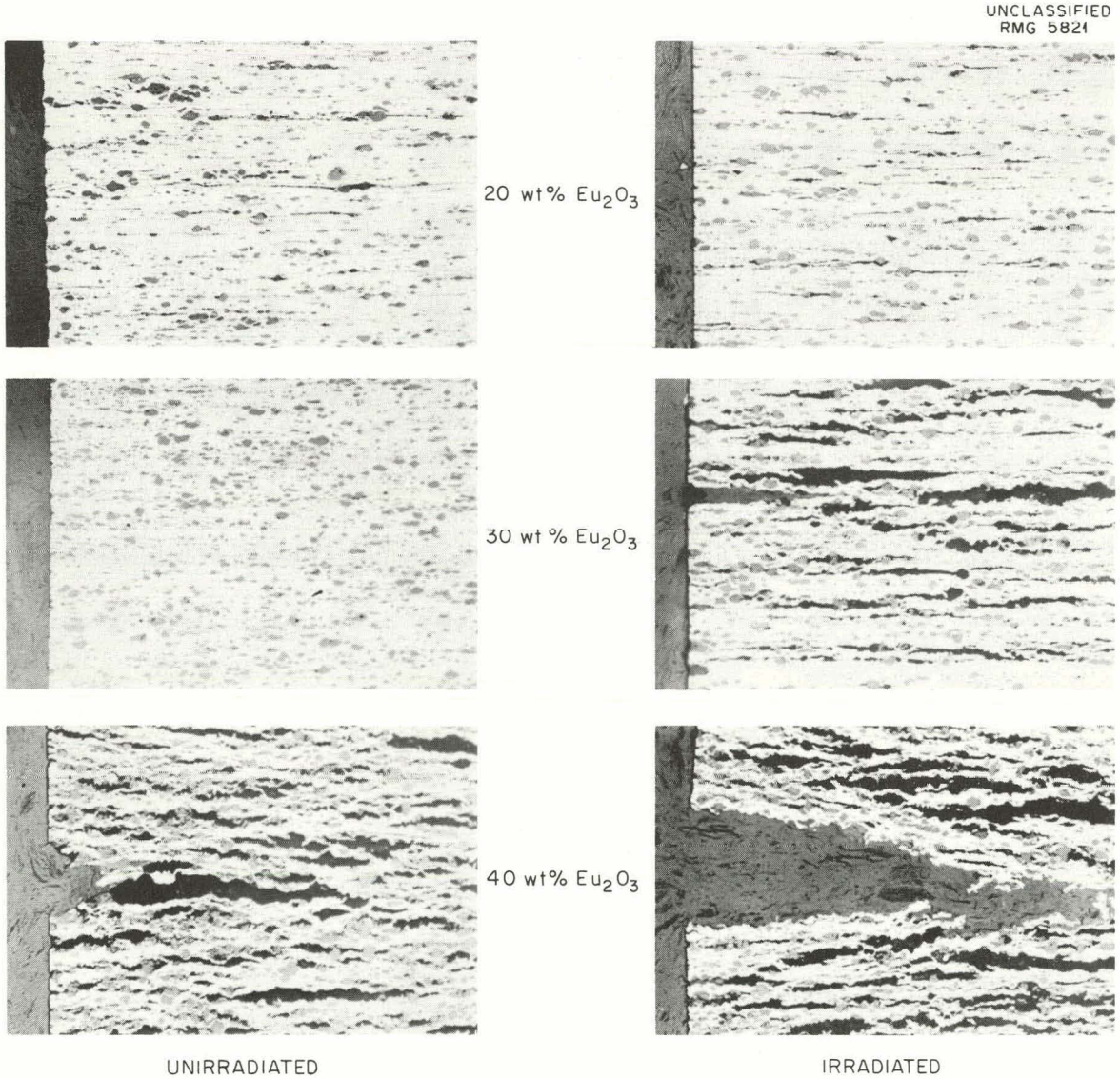


Fig. 5.8. Structure of Corrosion-Tested $Eu_2O_3$ Dispersion Absorber Specimens.

Table 5.2. Corrosion Test Results on Defected $Eu_2O_3$-Bearing Absorber Plates

| Irradiated Specimen[a] No. | $Eu_2O_3$ Concentration (wt %) | Weight Change (%) | | Thickness Change (%) | |
|---|---|---|---|---|---|
| | | Unirradiated Control | Irradiated Sample | Unirradiated Control | Irradiated Sample |
| 39-2 | 20 | +0.03 | +0.05 | 0 | 2.5 |
| 39-6 | 30 | 0 | +0.62 | 0 | 15.4 |
| 39-9 | 40 | +2.36 | +0.08 | 25 | 34.0 |

[a]Samples exposed to 300°C water for 88 hr.

splitting of the $Eu_2O_3$-stainless steel mixture. This effect appears to be a function of $Eu_2O_3$ concentration, since it was slight for the dispersion containing 20 wt % $Eu_2O_3$ but severe for the 40 wt % $Eu_2O_3$ sample. In comparison, only the unirradiated sample containing 40% $Eu_2O_3$ seemed to have suffered severe splitting. There is some indication, however, that the unirradiated specimen containing 20 wt % $Eu_2O_3$ was slightly affected. Comparative thickness changes caused by this corrosive attack are summarized in Table 5.2. These data show, as expected, large increases in thickness for samples containing 30 and 40 wt % $Eu_2O_3$. The exact nature of this phenomenon has not been discovered, but it is clear that dispersions containing 40 wt % $Eu_2O_3$, whether in the irradiated or unirradiated condition, are prone to deterioration when exposed to high-temperature water. Six specimens remain in-pile. The status of these irradiation experiments is summarized in Table 5.3.

Table 5.3. Status of Irradiations on $Eu_2O_3$-Bearing Miniature Absorbers (ORNL-MTR-39)

| Specimen No. | Accumulated Flux[a] (neutrons/$cm^2$) | Desired Flux (neutrons/$cm^2$) |
|---|---|---|
| | $\times 10^{20}$ | $\times 10^{20}$ |
| 39-3 | 21.8 | 28.8 |
| 39-4 | 27.4 | 45.7 |
| 39-7 | 24.9 | 28.8 |
| 39-8 | 27.8 | 45.7 |
| 39-11 | 26.2 | 28.8 |
| 39-12 | 24.3 | 45.7 |

[a]On July 17, 1961.

## Postirradiation Inspection of 17-4 PH Stainless Steel Control Rod Rack

K. K. Klindt  A. E. Richt
W. C. Thurber

In view of the stress-corrosion failures experienced at the Dresden Reactor in control rod components fabricated from 17-4 PH stainless steel,[11,12] the Oak Ridge National Laboratory was requested to examine a portion of one of the SM-1 control rod drives manufactured from similar material. The particular part to be examined was a multitooth shaft or rack approximately 41 in. long that had been exposed to the reactor coolant in SM-1 for approximately three years. During this period the plant operated at about a 50% load factor and the rack was exposed to dynamic 440°F pressurized water of neutral pH.

[11]Nucleonics, 19(1): 25 (1961).

[12]Nucleonics, 19(2): 25 (1961).


Fig. 5.9. Cross Section Through Tooth in 17-4 PH Stainless Steel Control Rod Drive Rack Showing Absence of Stress Corrosion After Extended Exposure to High-Temperature Water in SM-1 Reactor. Etchant: glycerol regia. 75X

In the hot cell, the rack was readily disassembled from its attachments. It was then subjected to visual inspection, followed by magnetic-particle and dye-penetrant surface examinations. No defects were revealed by any of these inspections.

Finally, the component was sectioned in several locations and examined metallographically to confirm the results of the nondestructive tests. The microscopic analysis confirmed the previous results. A typical section through one of the teeth in the rack is shown in Fig. 5.9; the integrity of the part is obvious.

The excellent service of this rack and six similar units is believed to result from the fact that these shafts were heat treated at 1000°F after fabrication to reduce residual stresses. Favorable water chemistry and the absence of boiling in the coolant may also have contributed to the satisfactory performance.

## 6. NOTCH-IMPACT TESTS OF SM-1 SURVEILLANCE SPECIMENS

R. G. Berggren M. S. Wechsler

Surveillance specimens of ASTM A-212, grade B, steel from the SM-1 pressure vessel were placed in the SM-1 reactor at startup. Eight capsules were placed on the core support plate 15.0 in. from the vertical centerline of the reactor with the bottom notch of the impact bars 16.7 in. above the core center. Each capsule contained three subsize Izod impact specimens with six notches each. Since there is a steep fast-neutron flux gradient in this position, each notch of a specimen was exposed to a different fast-neutron flux. One capsule was removed from the reactor after 16.4 Mwyr of operation, and tests were conducted on the impact specimens at ORNL. The exposure temperature of the capsule was about that of the exit coolant (450°F).

Notch 1 was farthest from the reactor core and, therefore, received the lowest fast-neutron dose. Notch 6 was nearest the reactor core but apparently did not receive the highest fast-neutron dose. Notch 5 appeared to receive the highest dose. There were three specimens in the capsule so that three tests were possible at each dose level. Unirradiated specimens from the same plate were tested in the hot cell along with the irradiated surveillance specimens.

The results of these tests are presented in Fig. 6.1. The increasing transition temperature with increasing fast-neutron flux or dose is apparent. The data for notch 2 show some scatter. The data point at 78°F and 5.2 ft-lb for notch 2 is suspect because of material inhomogeneity evidenced by a "step" in the fracture surface. The apparent anomaly for the notch 6 curve may be due to a spurious result for the test at 120°F or to a difference in exposure temperature. The observed transition temperature increases ranged from 36°F for notch 1 to 138°F for notch 5. Metallographic examination and radiochemical analysis are being performed on these samples.

Mockup experiments are being performed by Alco Products, Inc. in order to determine the relation of the fast-neutron flux at the SM-1

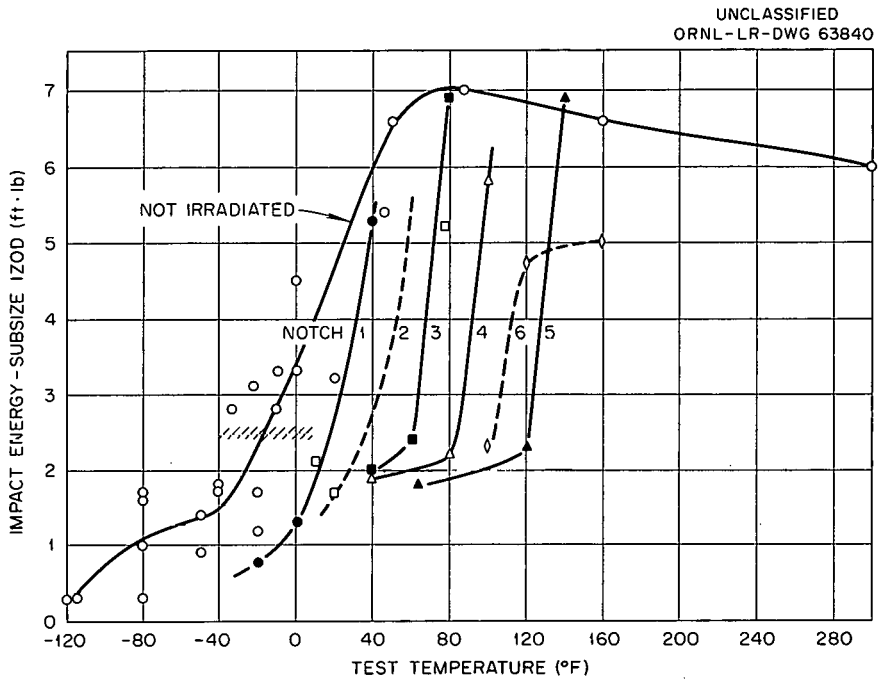


Fig. 6.1. Results of Impact Energy Tests on Surveillance Specimens of ASTM A-212, Grade B, Steel from SM-1 Pressure Vessel Material After 16.4 Mwyr in SM-1 Core.

reactor pressure vessel to the capsules in the reactor support structure. This work is not yet complete, but present estimates indicate that the maximum pressure vessel dose is comparable to notch 2 in the capsules. If this is substantiated in the final analysis, this will mean that the maximum transition temperature shift in the pressure vessel steel was 52°F at 16.4 Mwyr.

THIS PAGE

WAS INTENTIONALLY

LEFT BLANK

ORNL-3231

UC-80 – Reactor Technology
TID-4500 (16th ed.)

## Internal Distribution

1. T. D. Anderson
2. S. E. Beall
3. R. J. Beaver
4. M. Bender
5. R. G. Berggren
6. D. S. Billington
7. R. E. Blanco
8. E. P. Blizard
9. A. L. Boch
10. C. J. Borkowski
11. G. E. Boyd
12. R. B. Briggs
13. F. R. Bruce
14. D. W. Cardwell
15. J. H. Cherubini
16. T. E. Cole
17. B. W. Colston
18. W. B. Cottrell
19. J. A. Cox
20. F. L. Culler
21. J. E. Cunningham
22. E. P. Epler
23. W. K. Ergen
24. A. P. Fraas
25. J. H. Frye, Jr.
26. W. R. Gall
27. J. C. Griess
28. W. R. Grimes
29. E. E. Gross
30. J. P. Hammond
31. T. H. Handley
32. W. O. Harms
33. V. O. Haynes
34. M. R. Hill
35. W. H. Jordan
36. S. I. Kaplan
37. P. R. Kasten
38. O. H. Klepper
39. K. K. Klindt
40. R. B. Korsmeyer
41. P. G. Lafyatis
42. J. A. Lane
43. C. E. Larson (K-25)
44. G. W. Leddicotte
45. C. F. Leitten
46. R. N. Lyon
47. H. G. MacPherson
48. W. D. Manly
49. E. R. Mann
50. H. C. McCurdy
51. R. A. McNees
52. A. J. Miller
53. E. C. Miller
54. K. Z. Morgan
55. F. H. Neill
56. M. L. Nelson
57. W. R. Osborn
58. P. Patriarca
59. A. M. Perry
60. D. Phillips
61. R. A. Potter
62. M. E. Ramsey
63. A. E. Richt
64. J. T. Roberts
65. M. W. Rosenthal
66. A. F. Rupp
67. H. W. Savage
68. A. W. Savolainen
69. L. D. Schaffer
70. M. J. Skinner
71. G. M. Slaughter
72. A. H. Snell
73. I. Spiewak
74. J. A. Swartout
75. J. W. Tackett
76. W. C. Thurber
77. D. B. Trauger
78. T. D. Watts
79. A. M. Weinberg
80. M. S. Wechsler
81. C. L. Whitmarsh
82. M. L. Winton

83-85. ORNL Y-12 Technical Library Document Reference Section
86-120. Laboratory Records Department
121. Laboratory Records, ORNL R.C.
122-124. Central Research Library

External Distribution

125-126. Alco Products, Inc. (Attention: H. R. Clayton)
127-128. Alco Products, Inc. (Attention: J. R. Gallagher)
129. Alco Products, Inc. (Attention: K. Kasschau)
130-139. Division of Reactor Development (Army Reactors), AEC, Washington (Attention: W. C. Gribble)
140-141. Division of Reactor Development (Maritime Reactors), AEC, Washington (Attention: E. K. Sullivan)
142-143. The Martin Company, Nuclear Division (Attention: J. F. O'Brien)
144. New York Operations Office, AEC, New York (Attention: I. M. Adler)
145-147. Reactor Division, AEC, ORO (Attention: D. F. Cope)
148-149. Research and Development Division, AEC, ORO
150. Union Carbide Corporation (Attention: R. W. McNamee)
151-751. Given distribution as shown in TID-4500 (16th ed., Rev.) under Reactor Technology category (75 copies – OTS)